PAPER No. 5.

REFRACTION MEASUREMENTS IN AN ARID CLIMATE.

M.S. Brown

SUMMARY. To provide estimates of the refraction errors on the results obtained from the optical tracking cameras used at the Woomera Rocket Range, equipment to measure the vertical refractive index and temperature gradients has been developed. The refractive index gradient is measured with a portable optical refractometer which is capable of measuring changes in the refractive index of the order of 5×10^{-8}. Temperature measurements are made on a 150 foot radio mast by means of a system of thermopiles. The design of the equipment is described and results are given. Results are also given of a year's measurements of atmospheric refraction over a fixed sightline at Woomera.

1. INTRODUCTION.

During the past three years measurements of atmospheric refraction, refractive index gradient and air temperature gradient have been made at the Woomera Rocket Range in South Australia. The work has been confined to the lowest 150 feet of the atmosphere as measurements of temperature by means of radio-sonde equipped weather balloons provide sufficient information at higher altitudes for our needs.

Woomera is situated about 300 miles north-west of Adelaide, on the fringe of the arid zone which covers the greater part of South Australia. The climate is typical of much of the interior of Australia, with predominantely clear skies, low rainfall, high summer temperatures and a relatively cool winter period. The mean maximum shade temperature is above 32°C during the three summer months and drops to about 18°C in the winter. The diurnal variation of temperature is normally about 16°C. Average rainfall is 7 inches per year and the relative humidity at midday varies from near 20% in summer to around 50% in the winter.

In order to track the path of rockets launched from the range, kinetheodolites are used. These are a combination of theodolite and cine camera fitted with a long focal length lens. On each frame taken by the camera is shown the view through the lens, the azimuth and elevation angles along which the lens is pointing, and a frame number. The most accurate of these instruments are the Swiss made Contraves Kine-theodolites, which can measure angles to an accuracy of better than ± 20 seconds of arc. Measurements of atmospheric refraction and temperature gradients were started at Woomera so that corrections could be applied to the results obtained from these instruments. Also, the question arose as to the best time of day for taking measurements and the possibility of seasonal trends in refraction.

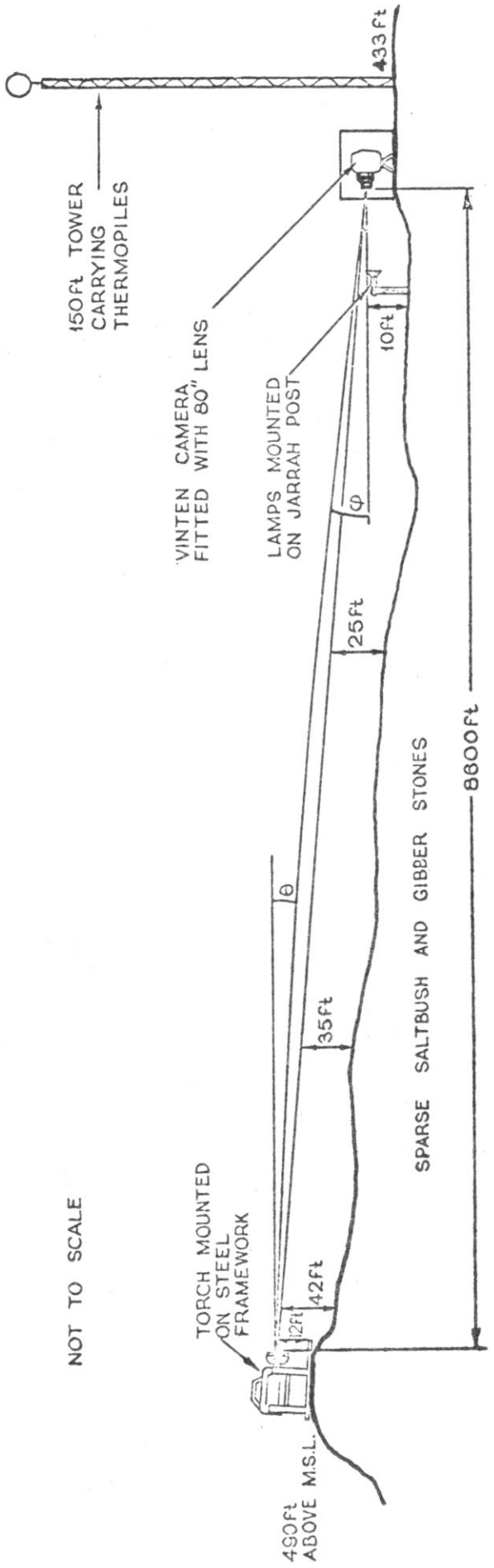

FIGURE 5.1. GENERAL ARRANGEMENT OF REFRACTION MONITOR AND TEMPERATURE RECORDING EQUIPMENT.

2. REFRACTION MEASUREMENTS.

Measurements of the diurnal change in the refraction angle had been made previously by ANGUS-LEPPAN (1963) in South Africa, using survey theodolites to take the readings. Also, in 1925 Johnson and Roberts measured refraction angles over a fixed horizontal sightline in Southern England by using a telescope to view two targets at distances of 362 metres and 724 metres. (JOHNSON and ROBERTS, 1925) The targets were marked with regular graduations, and by estimating the apparent relative positions of the targets they were able to calculate the difference in the refraction angle for the two sightline lengths.

In order to perform a continuous series of refraction readings, a similar experimental arrangement to that used by Johnson and Roberts was set up. Lamp targets were mounted 100 feet and 8600 feet from an automatic camera fitted with a long focal length lens and pictures were taken every 5 minutes day and night.

The general arrangement of the experiment and the terrain beneath the sightline are shown in Fig. 5.1

The lens used was a reflecting telescope of 80 inches focal length. The field of view was divided horizontally. The top half gave an image of the distant target. The lower half was fitted with a compensating mirror system so that the image of the near target was brought to the same focus as the image of the distant target.

The camera was triggered electrically from a timing circuit and took one frame approximately every 5 minutes. An electric clock was built into the camera and its face was imaged onto one corner of each frame to show when the frame was taken.

The camera, lens and timing circuit were housed in an air conditioned hut in which the temperature was maintained at about 21°C.

The equipment was calibrated by taking reciprocal elevation readings along the same sightline as the recording camera. The readings were taken in the morning and evening while the automatic camera was working. The refraction angle was the difference between the apparent elevation angle measured from one end of the sightline and the mean elevation angle computed from the reciprocal readings.

The calibration told us the distance between the two images of the targets for zero refraction angle. Knowing this figure the refraction angle for any other image separation could be found. The smallest movement we could resolve on the film was .001 inches which represents an angle of 2.6 seconds of arc.

The calibration was repeated every two months to avoid any errors due to movement of the near target.

Results. The graphs of the diurnal variation in the refraction angle (Figs. 5.2 and 5.3), show the average of readings taken during the first week of each month and the maximum and minimum recordings during that time. A group of 3 readings was taken every half hour day and night. The arrows beneath the graphs indicate times of sunrise and sunset.

No graph is given for January as the equipment could not be serviced during the Christmas vacation. The graph showing the range of diurnal refraction for each month (Fig. 5.4) is taken from the mean lines of Figs. 5.2 and 5.3.

Unfortunately, at the time these measurements were taken, no facilities for measuring the air temperature gradient were available. The weather information shown in Fig. 5.4 was obtained retrospectively from a weather station some thirty miles from the working area but in similar terrain.

The surprising thing about the results was that the diurnal variation of refraction was remarkably constant throughout the year. During the day the refraction angle was mainly between zero and 2 sec/1000 ft. with a minimum recorded in the two hours after midday. There was always a slow increase in refraction from about 3 hours before sunset until several hours after. Night time refraction angles were always between 5 and 10 seconds/1000 feet in clear weather, and there was often a marked peak in the curve for the readings taken at dawn. The refraction angle dropped from its high night time value after the sun had been up for about an hour.

Seasonal trends cannot be accurately gauged from a recording period as short as 15 months, but negative refraction angles were measured only in the heat of the day during summer. During the winter, refraction angles tended to be more positive for the whole 24 hour period.

A rainfall recording coincided with a reduction in the refraction angle measured at night, and produced a fall in the diurnal range of refraction. This result was expected, as it is well known that the presence of cloud cover reduces the diurnal range of temperature, and the magnitude of the temperature gradient. The graphs of rainfall and temperature range show some correlation with the graph showing the range of refraction, but they are really included only as an indication of the weather conditions under which the measurements were made.

An important conclusion from this survey is that refraction effects on horizontal sightlines 20 feet or so above the ground are small for the four hours about midday both in summer and winter. At night large refraction angles can be expected throughout the year.

We learnt quite a lot from our refraction measurements, but to provide estimates of refraction angles on sightlines at higher elevation angles it was necessary to know how the refractive index gradient varied with height.

3. REFRACTIVE INDEX AND TEMPERATURE MEASURING EQUIPMENT.

At the start of each trial, we already had a radio-sonde balloon released, which provided temperature information at intervals of a thousand feet or more up to a sufficient height for our needs. However, the weakness with these devices is that they provide no information about the first few hundred feet of the atmosphere, where quite considerable variations occur.

To fill in the gap, we designed equipment to measure the temperature gradient near the ground and mounted it on a 150 foot mast in the range area. We also measured the refractive index gradient directly, and while the refractometer which we constructed is not used for the routine work at the range, it proved such a useful and reliable instrument that a description of it is given here.

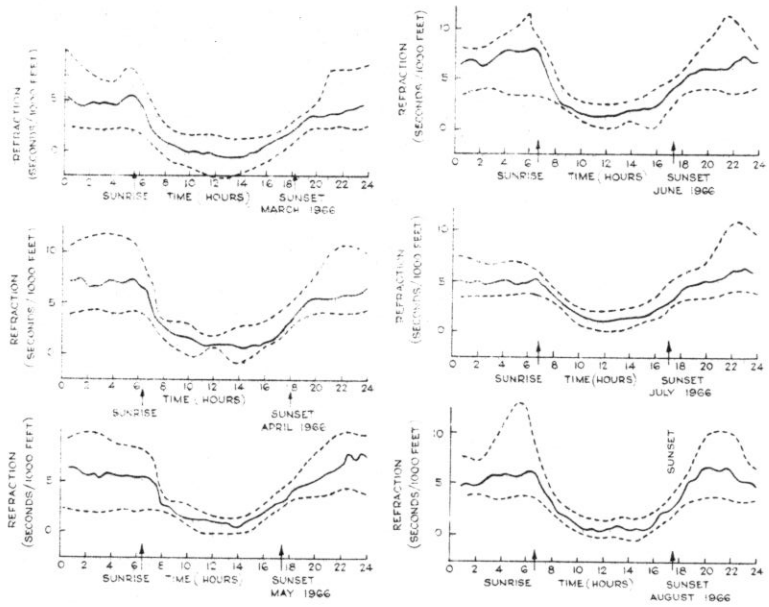

FIG. 5.2: DIURNAL VARIATION OF REFRACTION

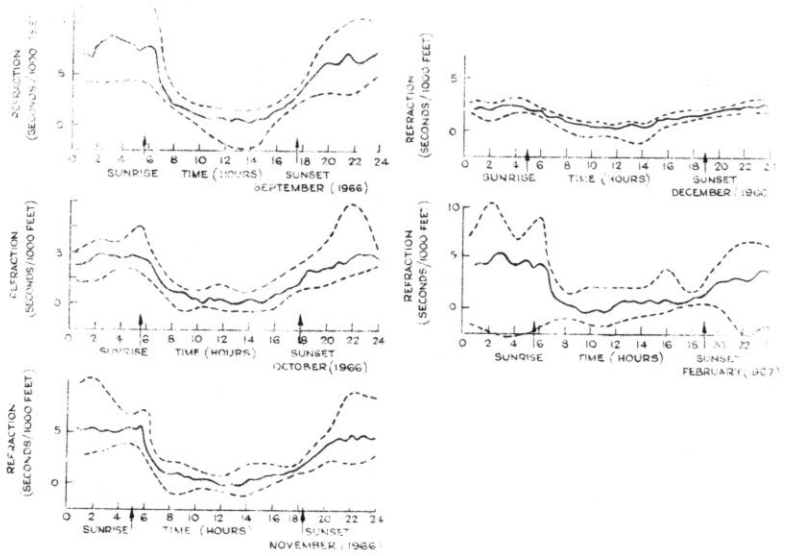

FIG. 5.3: DIURNAL VARIATION OF REFRACTION

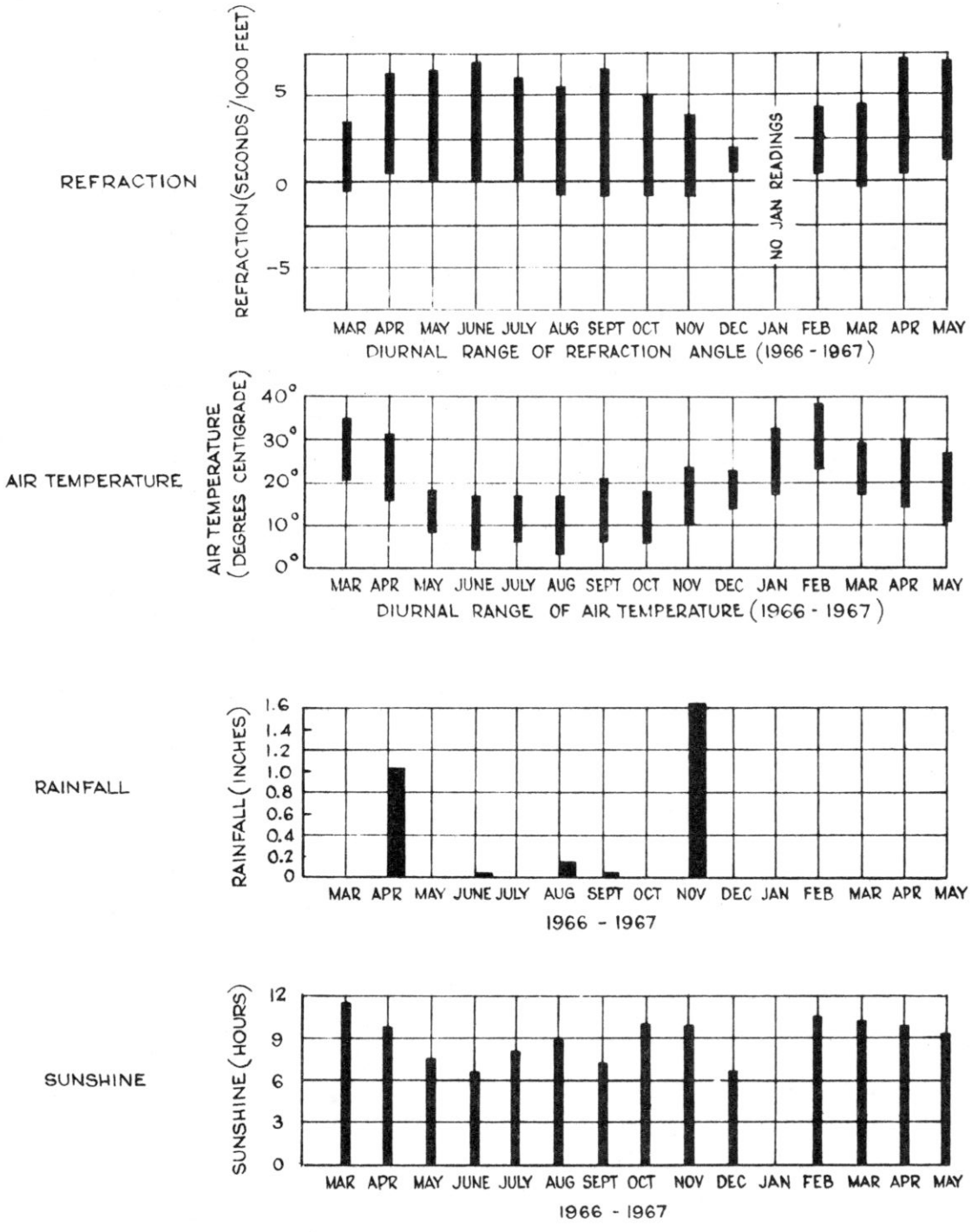

FIGURE 5.4. WEATHER INFORMATION DURING REFRACTION MEASUREMENTS

4. REFRACTOMETER DESIGN.

The interferometer arrangement used in the instrument was first described by Kosters (1931; SAUNDERS, 1957) and has been used more recently (TERREIN, 1965; SVENSSON, 1952).

The measuring system consisted of a two beam interferometer in which fringes at a suitable monochromatic wavelength were produced and photographed by a 16 mm camera. One beam passed through a vacuum chamber while the other passed through a similar chamber, filled with air, the refractive index of which was to be measured.

The path length through the vacuum chamber was L cm and the equivalent vacuum path of the air-filled chamber was nL, where n was the refractive index of the air. Thus the difference in path length between the two beams was

$$L(n - 1)$$

and the fringe shift caused by the introduction of the vacuum path $\frac{L}{\lambda}(n - 1)$ fringes. If the refractive index of the air changed by Δn then the interference fringes moved a distance $\Delta n . \frac{L}{\lambda}$ fringes.

The sensitivity of the refractometer is defined as the change in refractive index required to produce a movement of one fringe in the interference system. It is given by λ/L. The instrument used light of wavelength 5461Å and the sensitivity was 1.078×10^{-6} change in n per fringe.

The beam splitter (SAUNDERS, 1957B) consisted of two 30°, 60°, 90° glass prisms cemented together as shown in Fig. 5.5. The surfaces in contact were coated with a semi-reflecting aluminium film.

Collimated light from a mercury arc lamp entered one of the hypotenuse faces at normal incidence and was split into two beams by the aluminium film. The beams underwent total internal reflections at the hypotenuse faces and passed through the cell. A mirror reflected the beams back through the cell to the beam splitter, where they recombined and passed to the camera via a lens, aperture stop, and Wratten No. 58 filter. Both the collimator and camera optical system were folded by front aluminised mirrors to reduce the physical dimensions of the instrument.

The cell is shown diagrammatically in Fig. 5.5. It had two chambers, one of which was evacuated to a pressure of 10^{-3} mm mercury and the other was open to the atmosphere. The optical images of A and D (Fig. 5.5) coincide and the interference fringes produced are displaced by changes in the refractive index of the air. The images of B and C also coincide and the fringes formed are used as reference fringes.

Tilt fringes were introduced into the system by means of a wedge incorporated in one side of the beam splitter. The construction of the instrument is shown in Fig. 5.6

When in use, the cell assembly was supported only at the beam splitter end, and the instrument was pendulous with a natural frequency of 3/4 hertz. This method of assembly and suspension proved very satisfactory and the interference fringes were stable even when the equipment was being used in 25 mph winds. The refractometer was subjected to several hard knocks, intentional and otherwise, but no damage resulted and only slight adjustment of the interference fringes was necessary.

Camera System. The camera was a 16 mm cine magazine modified so that the film was driven at a constant speed. The complete field of view at the film plane is shown in Fig. 5.7a. To record fringe movements continuously, two slits were placed in front of the slowly moving film as shown in Fig. 5.7b. Half the film width was occupied by the reference fringes and the other half by the measuring fringes. Fig. 5.7c shows the effect on the film when the refractive index increases at a rate of 5×10^{-6} per second. In practice, much smaller changes occurred. When required, an event mark was recorded by illuminating the exit slits with white light from a tungsten filament lamp.

Measurements. The instrument measured changes in refractive index, not the absolute value. In practice the instrument was used to measure the change in refractive index as it was lifted in discrete steps above the ground, so that a picture of the refractive index gradient could be constructed. At various times we have used tethered balloons, a crane and a tall radio mast to lift the equipment.

Movements of the interference fringes which monitor refractive index were measured in relation to the reference fringes rather than the edge of the film. This eliminated errors due to instabilities in the mirror systems or distortions of the refractometer body which could cause the image-forming rays of both fringe systems to be deflected.

Fig. 5.8 shows some refractive index measurements made in the summer at Woomera. The day time recording shows the large refractive index inversion near the ground which gives rise to mirage effects. At night the gradient is larger with no inversion.

There were several sources of error in the instrument. The length of the cell changed due to thermal expansion and changes in the atmospheric pressure. The cell tended to distort due to uneven heating effects. The magnitude of these errors was normally small enough to be ignored. They are discussed in detail in Appendix I.

5. TEMPERATURE MEASURING EQUIPMENT.

Our temperature measurements are made on a 150 foot guyed mast which is situated about 10 miles down range from the launchers, in the centre of the area where the Contraves kinetheodolites are used. We chose a thermoelectric system for our measurements as suitable thermocouple wire was readily available and the electrical output from the system could be recorded easily.

Copper and constantan wires are used for the thermocouples. In order to produce an E.M.F. sufficiently large to be recorded by a pen recorder, twelve thermocouples are operated together to form a thermopile. A series of these is arranged up the mast to measure the temperature differences between heights of 5, 10, 30, 49, 68, 92, 116, 146 feet above ground. The junctions are positioned closer together near the ground where higher temperature gradients are encountered. In addition to the temperature difference measurements, the air temperatures at the top and bottom of the mast are measured by single copper constantan thermocouples referred to an automatic hot junction. This method of measurement gives good sensitivity for measuring temperature gradients but is somewhat inaccurate for measuring the air temperature. However we are mainly concerned with the temperature gradient.

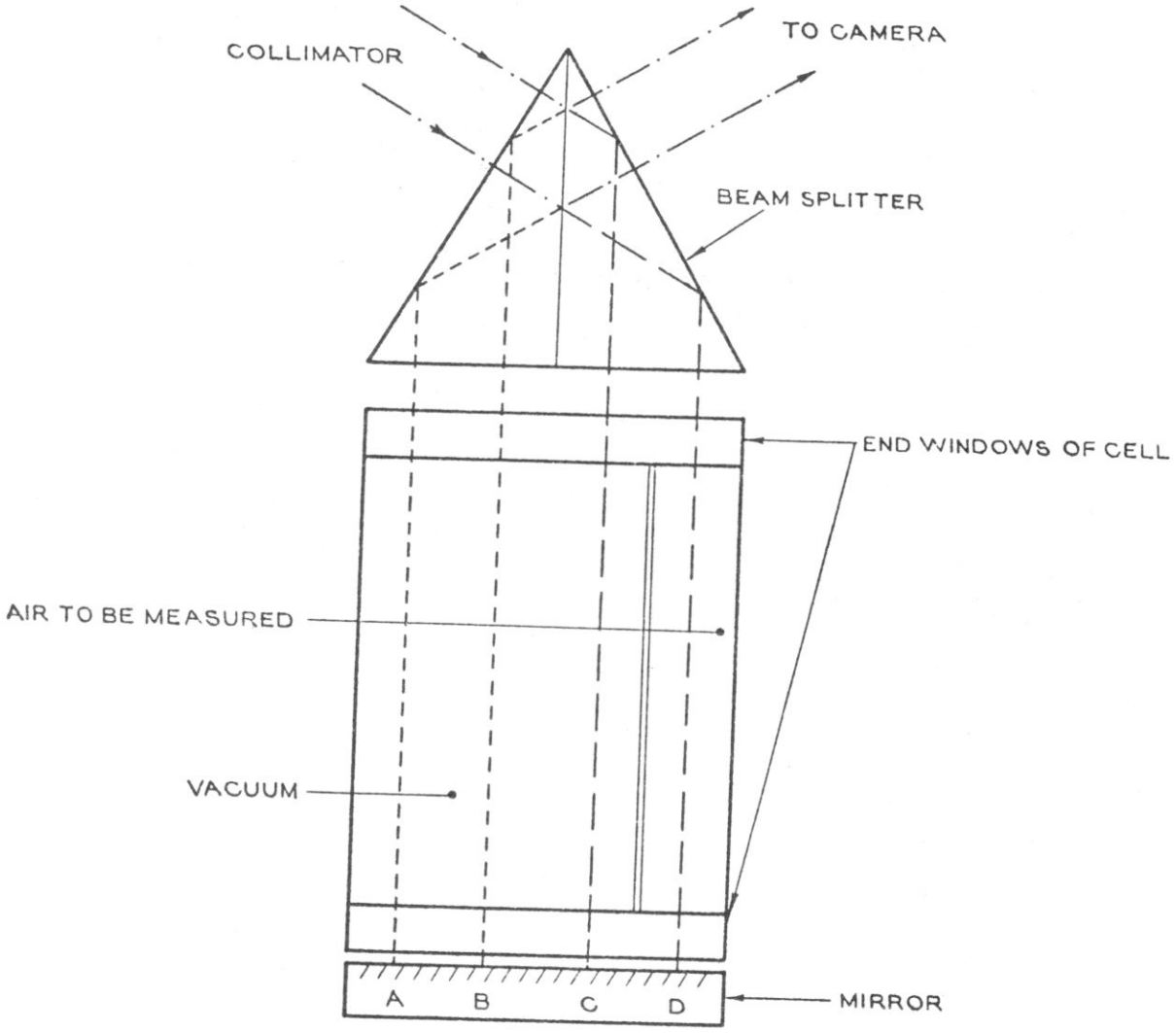

FIGURE 5.5. INTERFEROMETER ARRANGEMENT SHOWING THE INTERFEROMETER CELL.

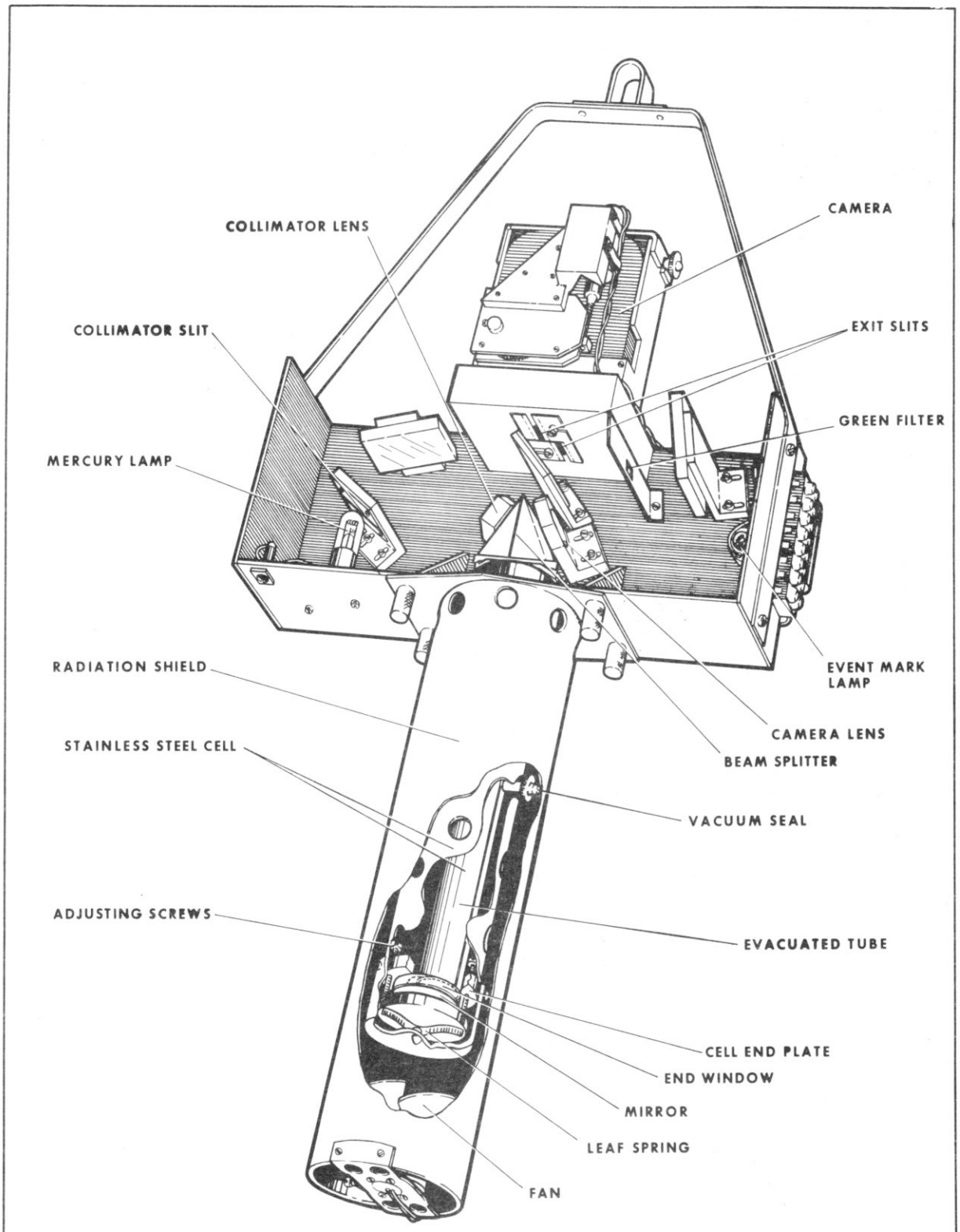

FIG. 5.6: GENERAL ARRANGEMENT OF REFRACTOMETER

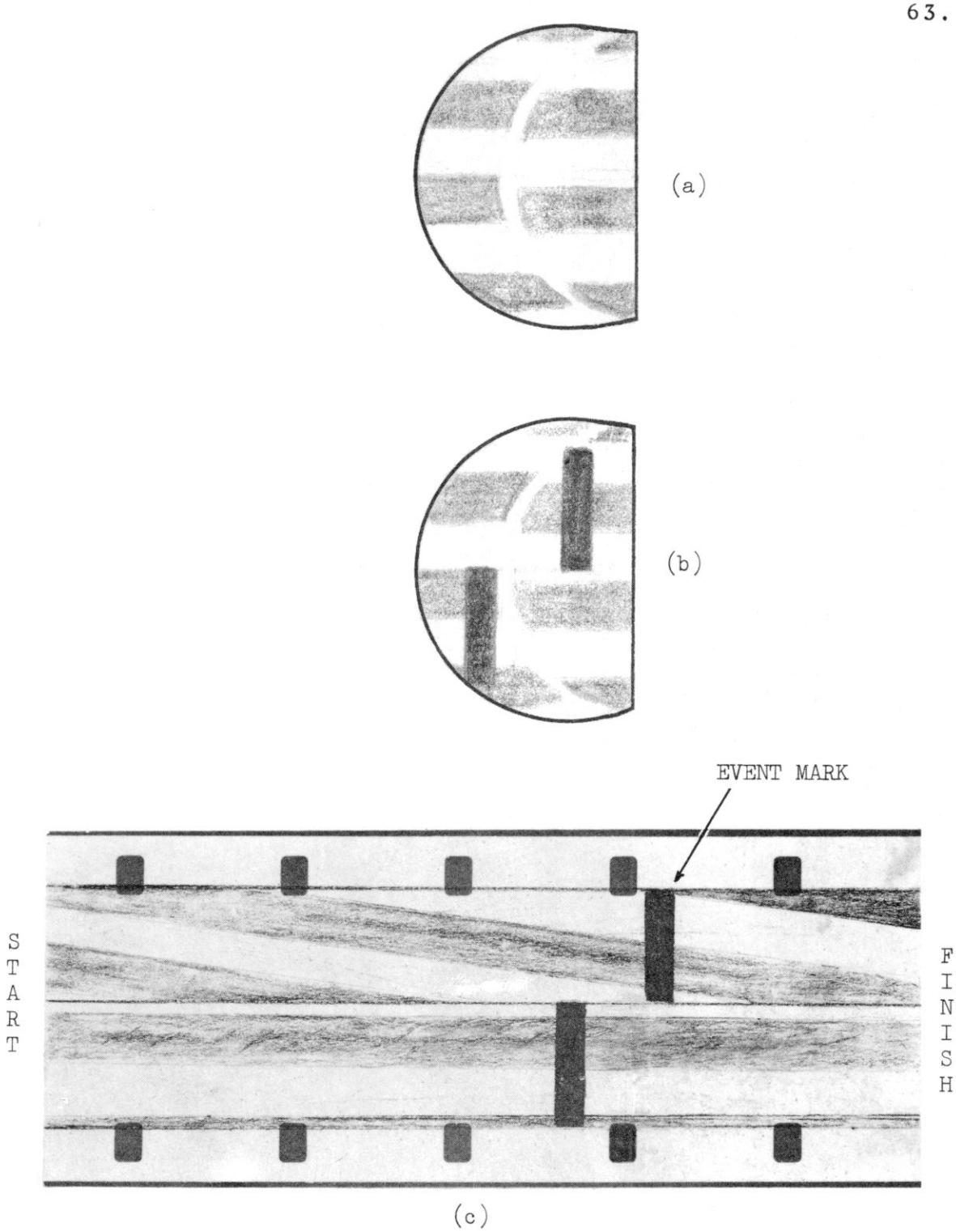

FIGURE 5.7. FRINGE MOVEMENT RECORDING SYSTEM.

The top and bottom junctions of adjacent thermopiles are enclosed in the same aluminium heat shield which consists of twin inverted aluminium cups mounted one inside the other, with a quarter inch air gap between them as shown in Fig. 5.9. Beneath the heat shield is mounted an electrical blower unit which creates an air flow of about 6 ft/sec. over the thermocouples. The air is exhausted through holes drilled in the sides of the radiation shields. Calculations on the heat dissipation of the motors have shown that negligible errors are introduced by proximity of the blower units to the thermocouples. The shield units are mounted 2 feet away from the tower on angle iron brackets.

Initial tests of the system indicated that the records would be confused by short time temperature variations during the day. To prevent this, damping was introduced into the system by adding a 2.5 gm brass heatsink to each thermocouple junction. The response time of the system was increased to about six minutes.

The recorder used is a 12 channel potentiometric strip chart recorder with a sensitivity of 2mv for full scale deflection on a 10 inch wide chart. Accuracy is ± 5% of full scale deflection.

6. DATA REDUCTION.

When the records are required for trials purposes, a still colour photograph of the pen recorder front panel is taken which shows the last 1½ hours of record. This forms part of the trials data which is flown down to Salisbury where the trajectory is computed. We are also doing a year's survey of atmospheric temperature gradients in the first 150 feet, so that refraction effects can be predicted. For this work, the records are removed from the recorder each week and read for a 10 minute period every 4 hours, day and night. The chart readings are read on a semi-automatic film reader, and the readings are put on IBM data cards. The temperature at each junction position is found by a summation process which adds each temperature difference reading to the temperature at the bottom of the tower. In the case of the temperature survey, cards are punched which show date, time and the eight temperatures up the mast. These are later used to compute the monthly mean temperature and temperature gradient, and the standard deviation about the mean gradient.

Some typical results from the temperature survey are shown in Figs. 5.10 and 5.11. Fig. 5.10 shows all the readings taken in August 1967, at 1200 hours. The mean temperature at each height is shown as the thicker line. A wide range of temperatures were measured at this time of the day, and we have found that similar scatter occurs at any time. Generally at one time of day the temperature gradient displays much less variation during the month than the air temperature. Fig. 5.11 shows the mean temperature gradients for the six measuring times together with the standard deviation.

Early indications are that temperature measurements taken at the mast when a trial is in progress can be used to provide refraction corrections for instruments which are operating several miles from the temperature measuring site. In an experiment to check this, we used a survey theodolite to measure the change in elevation angle of four lights at various positions on the range. The sightlines were all at near zero elevation angles, and varied in length from 22,000 feet to 55,000 feet. The refraction angle was calculated assuming that the curvature of the sightline was given by:

$$F = \frac{16.28P}{T^2} \left(.0104 + \frac{dt}{dh}\right) \text{ seconds of arc}$$

where P is the atmospheric pressure in millibars

T is the absolute air temperature (^{o}K)

$\frac{dt}{dh}$ is the temperature gradient in ^{o}C/foot

Some results from the experiment are shown in Fig. 5.12.

Although the temperature measurements were made on a treeless plain, and two of the sightlines were mainly over sparse woodland, the agreement between calculated and observed refraction was most gratifying.

ACKNOWLEDGMENT.

This paper is published with the permission of the Department of Supply, Australia.

REFERENCES:

ANGUS-LEPPAN, P.V. 1963 — A study of Refraction in the Lower Atmosphere. Survey Review, Vol. 16, Nos. 120, 121, 122.

JOHNSON, N.K. and ROBERTS, O.F.T. 1925 — The Measurement of the Lapse Rate of Temperature by an Optical Method. Quarterly Journal of the Royal Meteorological Society, Vol. 51, pp 131-138.

KOSTERS, W. 1931 — Interferenzdoppelprisma Fur Messzweeke, Reichspatentamt, Patentschrift NR 565211.

SAUNDERS, J.B. 1957A — The Kosters Interferometer. Journal of Research, National Bureau of Standards, Vol. 58, No. 1.

TERREIN, J. 1965 — An Air Refractometer for Interference Length Metrology. Metrologia, Vol. 1, No. 3.

SVENSSON, H. 1952 — Some New Interferometric Techniques and their Applications to Physico-Chemical Problems. Instruments and Measurements Conference Transactions, Stockholm.

SAUNDERS, J.B. 1957B — Construction of a Kosters Double Image Prism. Journal of Research, National Bureau of Standards, Vol. 58,No. 1.

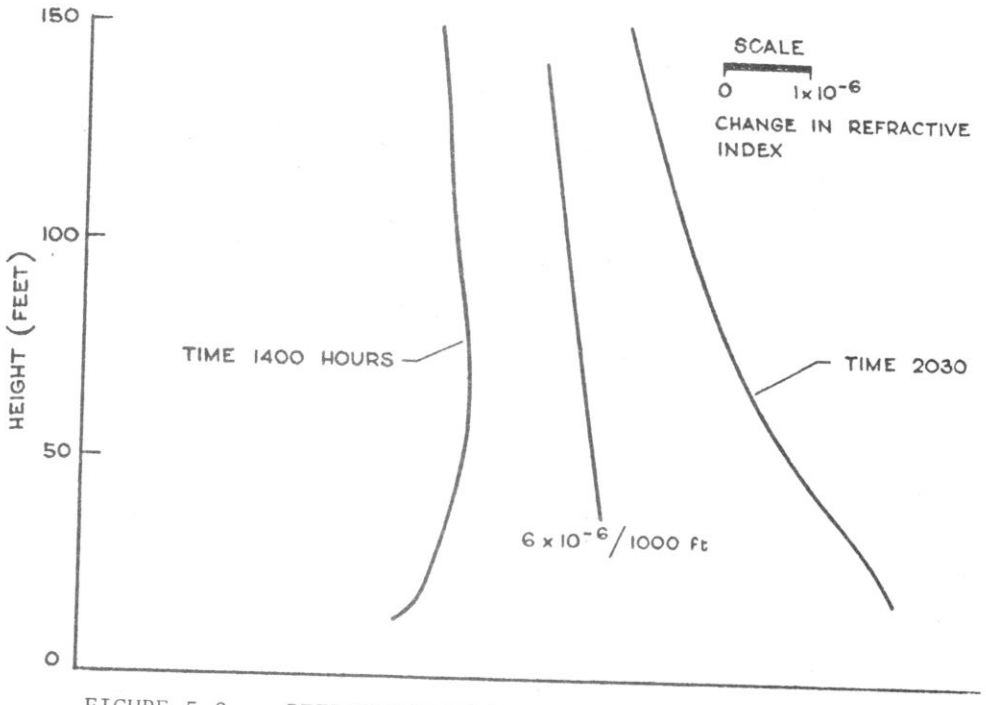

FIGURE 5.8. REFRACTIVE INDEX GRADIENTS MEASURED AT WOOMERA

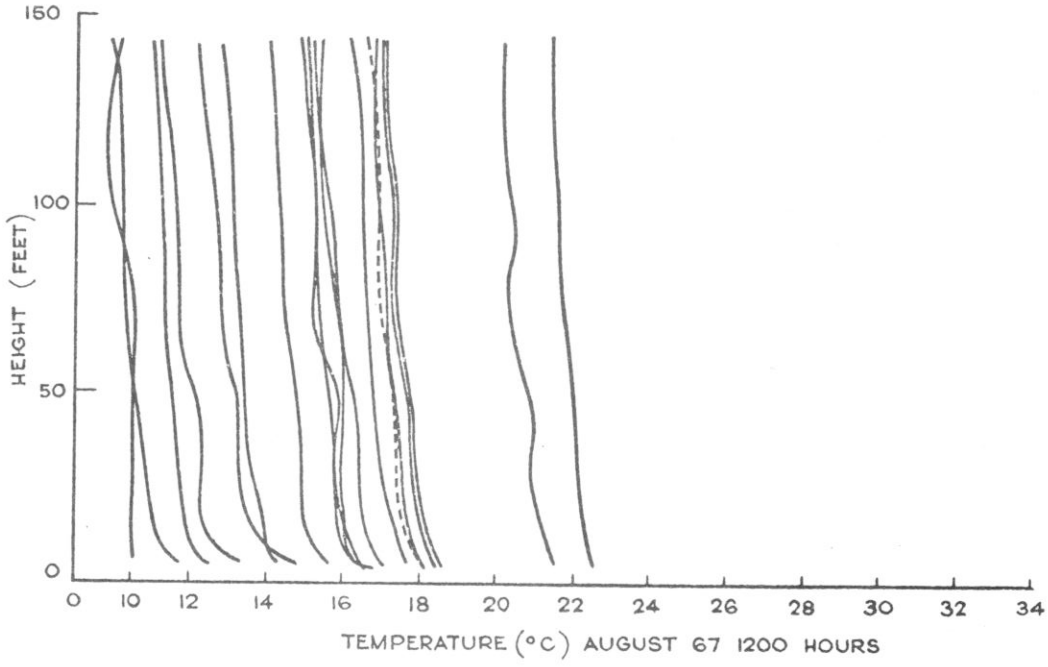

FIGURE 5.9. TEMPERATURE MEASUREMENTS MADE AT WOOMERA.

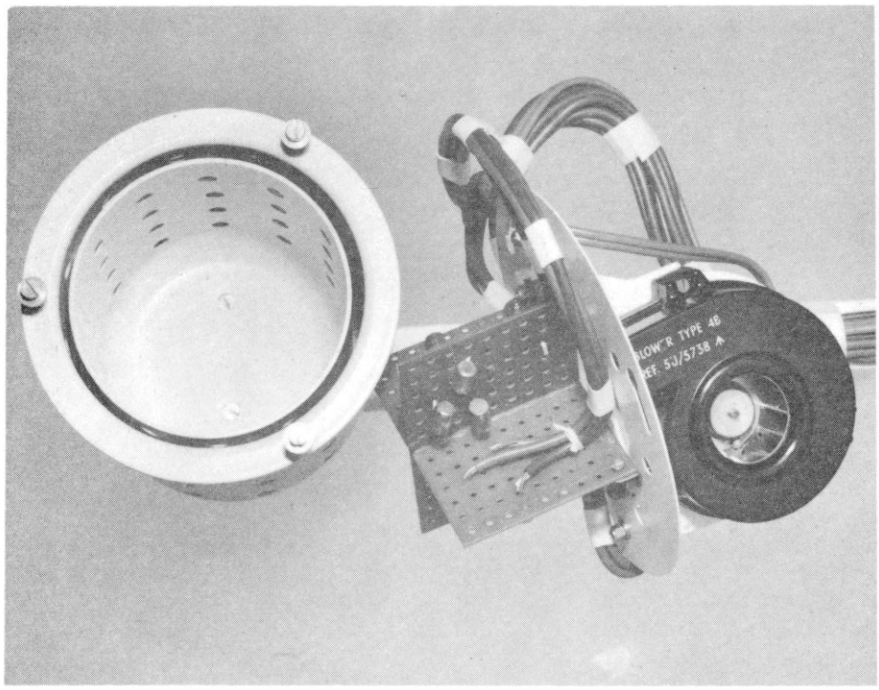

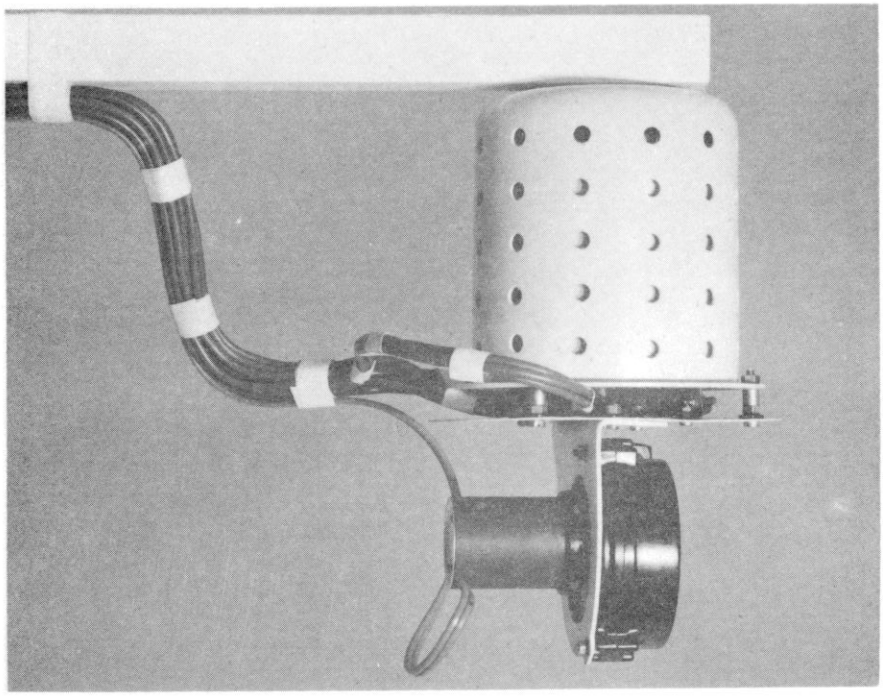

FIGURE 5.10. THERMOCOUPLE MOUNTING ARRANGEMENT

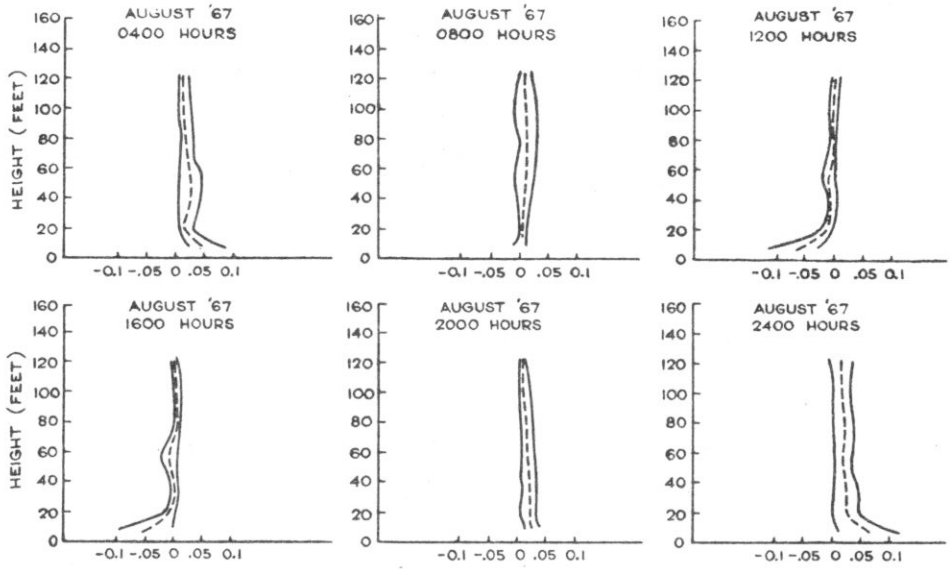

FIG. 5.11: MEAN TEMPERATURE GRADIENT AND STANDARD DEVIATION

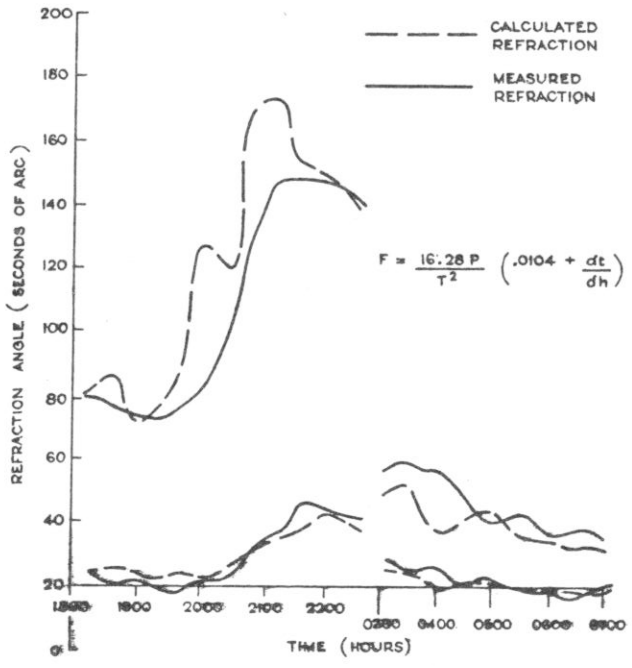

FIG. 5.12: MEASURED & CALCULATED REFRACTION ANGLES

APPENDIX I

SOURCES OF ERROR IN REFRACTOMETER.

CHANGES IN THE TEMPERATURE OF THE CELL. The difference in path length between the vacuum and air paths through the cell is given by

$$\frac{L}{\lambda}(n - 1) \text{ fringes}$$

When the temperature of the cell rises, the effective length increases by a factor of 10^{-5} per degree centigrade. Thus the path length difference alters by

$$\frac{L}{\lambda}(n - 1) \times 10^{-5} \text{ fringes}$$

When L = 50.72 cm λ = 5461 x 10^{-8} cm and n = 1.000292 the path length difference changes by 2.7 x 10^{-3} fringes per degree centigrade.

Since the resolution of the instrument corresponds to 1/20th of a fringe, this error is negligible.

AIR PRESSURE CHANGES AND THE LENGTH OF THE CELL. A height rise of say 500 ft produces a pressure reduction of about 16 mb, which causes a reduction in stress along the cell of 16 x 10^{-3} dynes/cm^2. Assuming that the young's modulus of the steel cell walls is 20 x 10^{11} dynes/cm^2 the change in strain along the cell is 8.3 x 10^{-9} For a cell length of 25.4 cm this amounts to a change in length (ΔL) of 21 x 10^{-8}cm.

Thus the fringe shift produced by the pressure reduction is $(n - 1)\frac{\Delta L}{\lambda}$ = 1.22 x 10^{-7} fringes, which may safely be ignored.

DISTORTION OF THE CELL. When the cell bends, the fringe system rotates, and the fringe spacing alters. This is recorded on the film as a movement of both the reference and the measuring fringes. Thus it is possible to reject those records where it occurs. In fact providing the refractometer is allowed half an hour to warm up to the ambient air temperature, no serious cell bending occurs.

If the refractometer is allowed to swing violently about its suspension point, the cell distorts and a slight wavering of the film record is produced. Normally the drag of the power supply cables is sufficient to damp out any such oscillations.

PRESSURE REDUCTION DUE TO FAN. The action of the fan which draws air through the cell causes a slight depression of the air pressure in the refractometer. The air flow has been kept as slow as possible but there remains an error of 1/6 fringe between "fan on" and "fan off". All readings are therefore taken with fan on.

PAPER NO. 6.

SURFACE EFFECTS ON REFRACTION IN PRECISE LEVELLING.

P.V. Angus-Leppan

SUMMARY. Atmospheric refraction, especially in the lowest layers, is affected by the type of surface. Refraction over ice is an extreme case. Special apparatus and experimental procedures have been designed to study this case, in the atmospheric layers which affect precise levelling. The results indicate very high values of the coefficient of refraction, and large variations with time. The same measuring procedures are applicable over other surfaces and some preliminary results are discussed.

1. INTRODUCTION.

The refraction of light rays through the atmosphere depends mainly on the temperature gradient, which in turn is greatly affected by the thermal properties of the surface. The influence of the surface is of course greatest in the lower layers and diminishes upwards.

During the day, under normal conditions, the sun's rays do not heat up the air in passing through, but heat the surface, which transmits heat upwards by convection. The temperature is highest at the surface, decreasing upwards, and the temperature gradient is negative. At night the surface cools off rapidly and the gradient becomes positive.

Conditions over ice or snow are very different as it is impossible for the surface temperature to increase above $0^{\circ}C$. Yet in summer the temperature even a few feet above the surface may be several degrees warmer, indicating a high value of the temperature gradient, and extreme bending of the light rays, through refraction.

These considerations led to the author's interest in the refraction over an icefield. An opportunity arose to take measurements during the Summer Institute of Glaciological and Arctic Sciences on the Juneau Icefield, Alaska, in 1966.

2. ICEFIELD EXPERIMENT, 1966.

The site of the experiment was between survey station 19, at Camp 10, and 20A, on a spur of Shoehorn Peak, 5701 metres distant. To cover a wider range

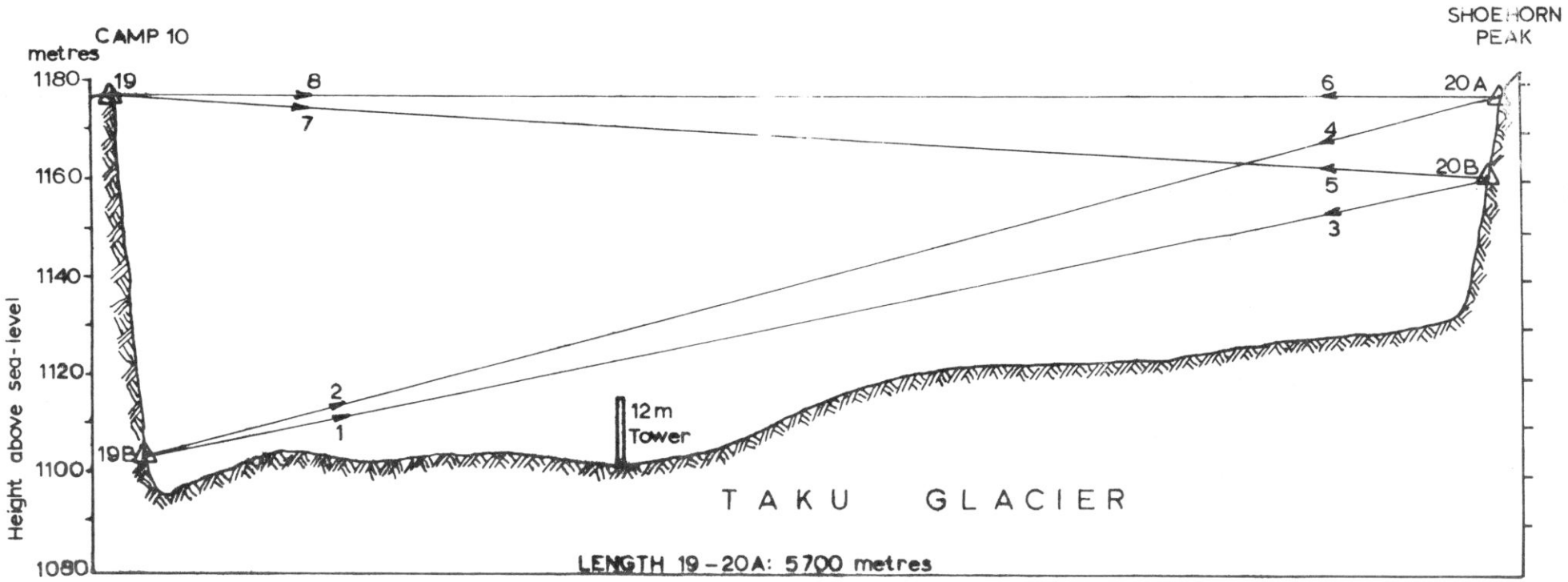

FIG.6.1 PROFILE SHOWING THE OBSERVING STATIONS, LINES OF SIGHT, AND TEMPERATURE IN RELATION TO SURFACE.
HORIZONTAL SCALE 1/20000, VERTICAL SCALE 1/1000

of heights an additional station was chosen at each end, giving the four lines shown in Fig. 6.1 which range from 15 to 70m. above the surface. The lines are over a smooth section of the Taku Glacier with a slight downward slope towards the Camp 10 end.

At approximately two-hour intervals vertical angles were measured from each station to the two stations at the far end. They were so arranged as to be simultaneous reciprocals between the two upper stations, then between the two lower stations, at alternate hours. Two Wild T2 theodolites were used for the angle measurements. The sighting targets were kerosene pressure lamps during the night and large orange squares of cotton cloth during the day.

Temperature measurements were made on a 12-metre tower which was situated along the line of sight and roughly midway between the ends. The temperature element was a small rod thermistor of the type used in radiosonde apparatus, coated to eliminate heating by radiation. Once every hour this was raised and lowered, with a pause at each of six measuring heights to allow sufficient time for the element to take up the air temperature, before recording the resistance.

Observations extended over a 24-hour period. The weather during the experiment was stable, being almost entirely cloudless, with light winds.

3. REDUCTIONS.

In order to compare the results from both angle and temperature observations, each type was reduced to the form of a coefficient of refraction.

For the angle measurements, K is the coefficient of refraction, defined as the ratio of the radius of the earth to the radius of curvature of the line of sight.

$$K = \frac{R}{R'} = \frac{R}{\frac{S\rho}{\theta+\alpha_1+\alpha_2}} \qquad \ldots.(1)$$

where α_1, α_2 are the observed angles of refraction at the ends of the line of sight, whose length is S and which subtends an angle θ at the earth's centre. ρ is the conversion factor from radians to seconds = 206265".

$$\theta = \frac{S\rho}{R}$$

$$\text{so that } K = 1 + \frac{R}{S\rho}\ (\alpha_1 + \alpha_2) \qquad \ldots.(2)$$

The practical value of K is that it facilitates the application of a correction for earth curvature and refraction in the form: $\frac{(1 - K)S^2}{2R}$, in units of S and R.

For the temperatures, curvature of the line of sight at a point is given by

$$F = 16.5\ \frac{P}{T^2}\ (0.034 + \frac{dT}{dz})$$

where F is in seconds per metre.

P is atmospheric pressure in millibars.

T is temperature in ^{o}K and

z is the height above the surface in metres.

Since the curvature $F = \frac{\rho}{R}$, Eq. (1) can be applied, so that, with appropriate values for P and T

$$K = \frac{RF}{\rho} = .205 + 6.15 \frac{dT}{dz}$$

Combined results are shown in Fig. 6.2 The relationships between K and the height and time are shown in the form of contours of equal coefficient of refraction K. Tracing along any horizontal line will give the time variation of K at that level, while values along any vertical line show the variation with height at the particular time.

The upper half of the figure, above 14m., is derived from angle measurements and confirms that there is no marked diurnal pattern at these levels. Above 40 m. the variations are comparatively smooth and regular, while below this level there are more marked irregularities. Even at these elevations above the surface, values of K are very much higher than the standard value of 0.14.

The lower half of the figure is derived from temperature measurements. Even allowing for the fact that these are point measurements as opposed to means over the length of a line of sight, it is clear that the pattern is different. The substantially horizontal trend of isolines gives way to a vertical trend with 'globules' of very high refractive index in the layer 2 - 10m., falling off again below 2m. to lower values. High values of K, up to 3.0,are found.

The lower level results, derived from temperatures, provide independent confirmation of the higher results. The two sets give numerical values which are consistent along the boundary level of 14m, and each increase or decrease along the 18m. level has a corresponding, though magnified, variation at the 10m. level.

The conclusions to be drawn from the measurements are that, as was to be expected, the refraction above a frozen surface is markedly different from refraction over a normal surface. The values of the coefficient of refraction K are remarkably high. In general the higher values are found near the surface and there is a decrease upwards. However even at the highest levels of measurement the values of K do not reach the normal values around 0.12 - 0.14. It appears rather that a value of 0.35 is appropriate for lines which do not graze the surface.

The general trend of decreasing K with height does not hold for the layer 2 - 10m, where the highest values, up to 3.0, were measured. This is apparently a transition zone in which high gradients are encountered between the lowest layer in contact with the cold surface, and higher, and warmer layers where winds perform more efficient mixing.

Another feature is the lack of any discernible diurnal cycle in the observations. This might be expected at higher layers, but even at the lowest levels it was absent.

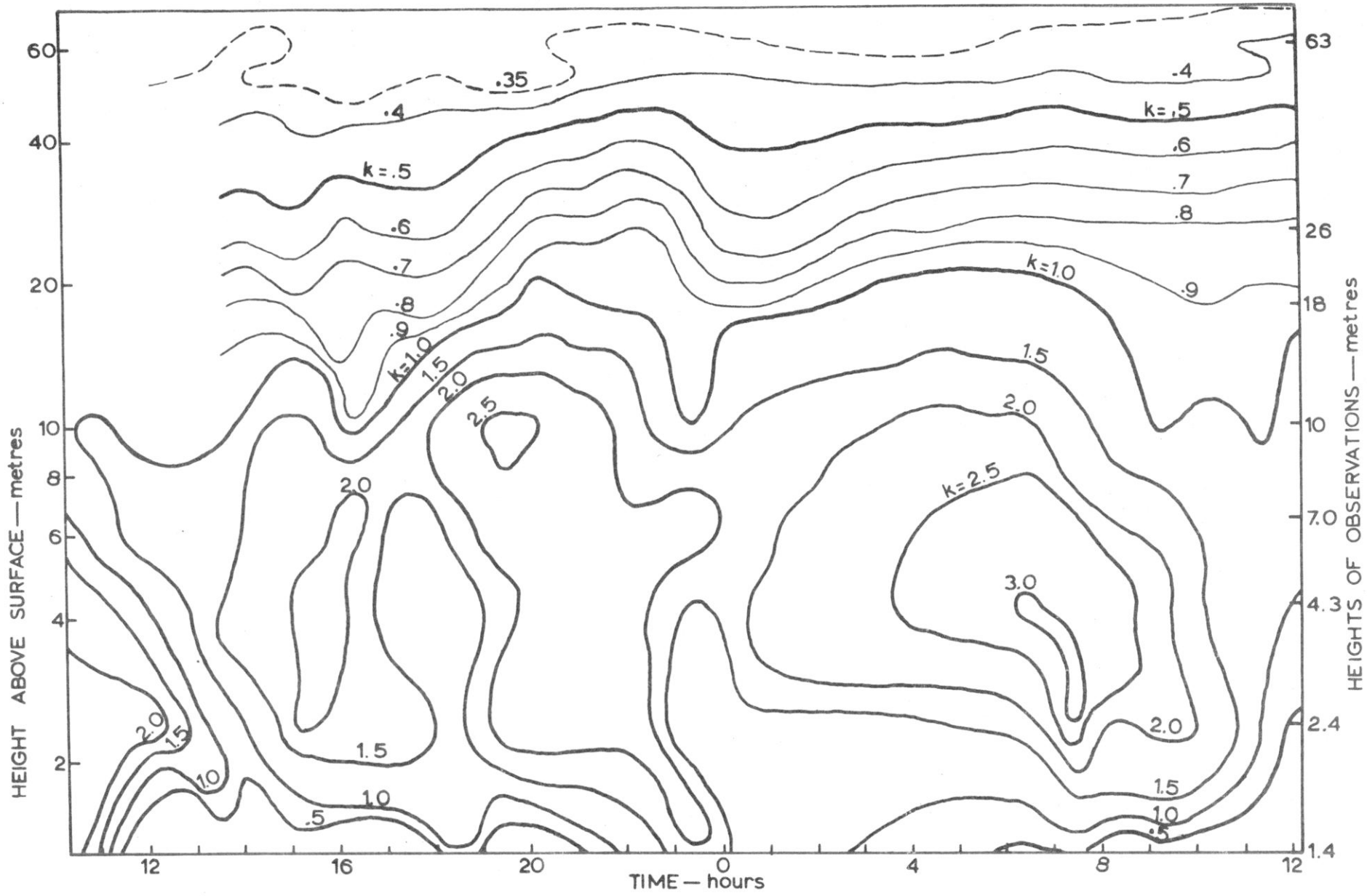

FIG. 6.2 COEFFICIENT OF REFRACTION DETERMINED FROM VERTICAL ANGLE AND TEMPERATURE OBSERVATIONS. VARIATION WITH HEIGHT AND TIME INDICATED.

The reason appears to be the constant high gradient and absence of convection even during the day, again a consequence of the constantly cold surface. The experiment is described and discussed in greater detail in another publication (ANGUS-LEPPAN, 1968).

4. ICEFIELD EXPERIMENT, 1968 - RECIPROCAL LEVELLING.

The 1966 experiment pointed to the necessity for two further studies: a more detailed study of the lower layer 0 - 4m, and a study of a layer extending considerably higher, 0 - 500m. When a further opportunity arose in 1968, the first of these two possibilities was chosen, partly due to practical limitations, as all apparatus had to be air-freighted from Australia to Alaska. It is also of practical significance. Many observations are taken over snow and ice, and there is a real possibility of large systematic and random errors.

In the well-known reciprocal levelling method of river crossings (Fig. 6.3), the relative elevations can be determined and refraction is eliminated. The same observations can also be used to calculate the refraction. The disadvantage on an icefield is that each staff and each level will be sinking into the ice at an unknown rate. In effect, there are only two independent observations, but six unknowns to be determined: the relative heights between levels and staves (three), the collimation error of each level (two), and the refraction (one). After trying and discarding schemes with multiple levels and staves in order to increase the number of useful observations, a simple method was devised to reduce the number of unknowns to two. The staves were replaced by short scales attached to the levelling instruments, whose collimation errors were determined. With no change in relative heights of instrument and staff, this left only two unknowns, the refraction and the relative height between the levels. The short length of the scales does not constitute a disadvantage, as the reciprocal lines of sight should in any case be at approximately the same elevation. If the collimation corrections of the two levels are equal but of opposite sense, the effect will cancel when determining the refraction, as shown below.

Due to the unstable surface it was essential that the levels should be of the compensator type: Zeiss N12 automatic levels were used, fitted with scales approximately 15 cms in length beside the telescopes. Standard parallel plate micrometers were attached. Since the normal "two-peg" adjustment is seriously affected by refraction errors, a theodolite telescope, set to give the horizontal, was employed as a collimator, enabling Level A to be adjusted to make its line of sight horizontal. The two levels were then set on a short rigid plate and the telescopes collimated into each other. On looking through each telescope an image of its crosshairs is seen, as well as a fainter image of the crosshairs of the other telescope. It is essential that each telescope should be focussed for infinity. The parallel plate micrometer provides a good check: when moved it should not cause any relative movement between the images of the crosshairs. In this position the crosshairs of Level B are adjusted so that the crosshairs of both instruments coincide. If Level A has a collimation error c, Level B will have an error (-c). The levels were tested by the same procedure before and after each daily set of observations.

In Fig. 6.4 the elevation difference between the height of collimation of the

level, A, and the zero F of the staff, is given by:

$$H_F - H_A = BD + DE - BC - CF = -EF$$

$$= Sc + \frac{S^2}{2R} - \frac{KS^2}{2R} - h_F$$

where c is the collimation error in radians.

The elevation difference between the two staves is given, from readings at Level 1, by,

$$(H_F - H_A) - (H_B - H_A) = H_F - H_B$$

$$= (S_L - S_S)c + (S_L^2 - S_S^2)\ \frac{(1-K)}{2R} - h_{F1} + h_{B1} \qquad \ldots.(3)$$

The symbols relate to Fig. 6.3.

H - elevation above datum

h - staff reading

Suffixes F, B - refer to foresight, backsight.

Suffixes 1, 2 - refer to observations with Level 1, Level 2.

Similarly, from observations at Level 2 with collimation error (-c)

$$H_F - H_B = (S_S - S_L)\ (-c) + (S_S^2 - S_L^2)\ \frac{(1-K)}{2R} - h_{F2} + h_{B2} \qquad \ldots.(4)$$

Equating (3) and (4), the collimation terms cancel, and the effect γ of curvature and refraction in terms of staff readings is given by

$$\gamma = (S_L^2 - S_S^2)\ \frac{(1 - K)}{R} \qquad \ldots.(5)$$

$$\gamma = (h_{F1} + h_{B2}) - (h_{B1} + h_{F2}) \qquad \ldots.(6)$$

Since S_S is, at most, one-tenth of S_L , $(S_L^2 - S_S^2) \simeq S_L^2 = S^2$, within 1%, (5) becomes $\gamma \simeq \frac{S^2}{R}(1 - K)$

Whence $K = 1 - \frac{R\gamma}{S^2}$ .... (7)

Using scales on the levels instead of staves, h_{B1} and h_{F2} become the readings on the scales equivalent to the heights of collimation, which can be determined by calibration.

It is only necessary to make reciprocal readings in circumstances where there is no appreciable refraction, that is, when $\gamma = 0$. With levels set at minimum focussing distance, about four metres, each level reads the scale on the other and the effects of curvature and refraction will be negligible. If the height of collimation of A is d above that of B,

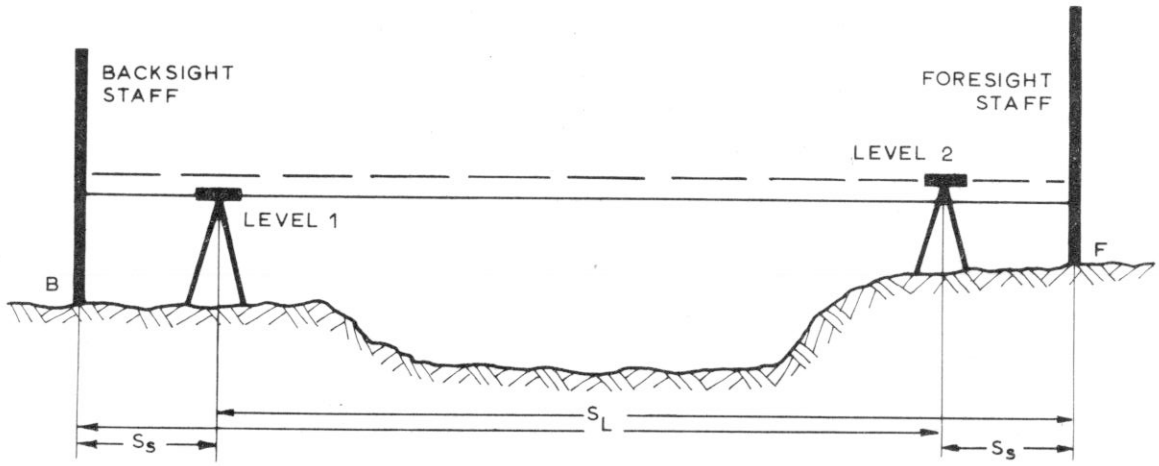

FIGURE 6.3: PRINCIPLE OF RECIPROCAL LEVELLING

Refraction eliminated by observing with both levels
Collimation error eliminated by reversing positions of levels

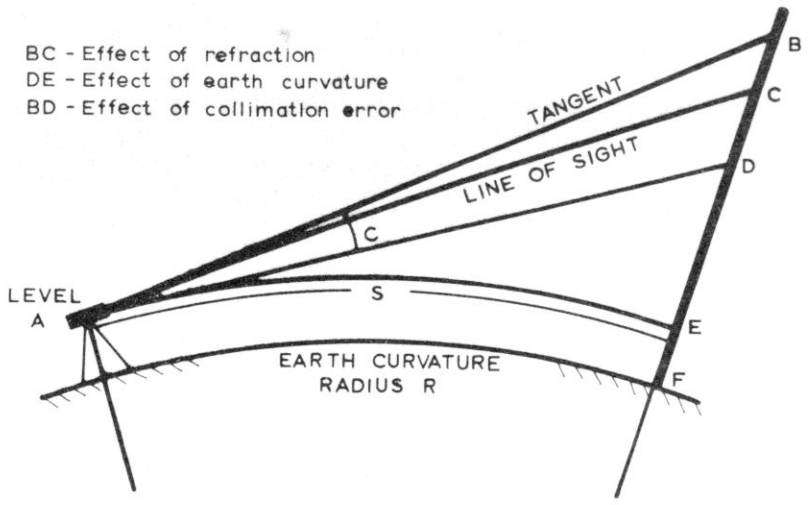

FIGURE 6.4: LINE OF SIGHT AFFECTED BY REFRACTION AND COLLIMATION

Height of collimation of A = $n_1 + d$,

where n_1 is the reading on A's scale observed through level B.

Similarly,

Height of collimation of B = $n_2 - d$.

It is not necessary to determine d since the calibration constant is the sum of these two collimation heights.

$$n_1 + d + n_2 - d = n_1 + n_2$$

Thus $\gamma = h_{F1} + h_{B2} - (n_1 + n_2)$ and K can be determined from (7)

Field measurements lasted normally from sunrise to sunset. After checking and, if necessary, adjusting the collimation, and making calibration measurements $(n_1 + n_2)$, a set of reciprocal scale readings was made every half hour, taking the usual precautions with the level. To increase precision and provide an estimate of the short-term variations, eight to twelve micrometer settings were made. Observers changed ends half-way through each set. The distance between levels was 60 - 70 m. The line of sight was approximately 1.6m above the surface. On the final day of observations a third N12 level became available, and was used to measure refraction on an additional line of sight .8m above the surface.

5. ICEFIELD, 1968 - TEMPERATURE GRADIENT.

Direct measurements of air temperature present difficulties because of rapid fluctuations with time, the air's low specific heat compared with the thermal capacity of the sensing element and the resultant danger of errors due to heat radiated or conducted to the element. If the element is aspirated and radiation shielded, the presence of the apparatus, the air movement due to aspiration and heat from the aspiration fan could all disturb the temperature structure which is the subject of measurement.

Apparatus was designed to avoid these sources of error as far as possible. The sensing element was a rod thermistor, which provides a compromise between the requirements of low thermal capacity and large surface area to take up the air temperature, and sufficient mass to damp out short-term variations. This was shielded from radiation in the centre of a double aluminium sleeve, the inner tube of which was connected to a funnel-shaped section leading to the aspiration fan. The fan motor was small and did not form a significant heat source. Air was sucked past the thermistor at about 12 feet per second. Five such aspirated thermistor housings were clamped in a horizontal position on a timber post 4 m. long, with the openings pointed upwind.

The high temperature coefficient of the thermistors kept the measuring apparatus comparatively simple. An off-balance bridge was built, with a number of ranges, each covering $10^{o}C$. Balance was set at the centre of the range of a micro-ammeter graduated from zero to ten, so that readings could be made directly in degrees. Standard resistances were built in for calibration of each range of the instrument.

Temperature observations were also made every half-hour, in conjunction with the refraction readings. A set commenced with the calibration readings, followed by a reading of each thermistor, from the lowest upwards, then down-

wards. Wind velocity was recorded in conjunction with the temperatures. Indications are that temperatures are observed to a precision of 0.1°C, though they are subject to fluctuations of a greater magnitude.

Besides the observations over the icefield where the surface was in fact firn (or old snow), limited observations were also made over mown grass and over asphalt surfaces in New South Wales. It is intended to continue these measurements over a number of typical surfaces. Details of the observations are given in Table I.

The various observing sites provide a range of surface conditions and climates. The Lemon Creek Glacier is close to the southern edge of the Juneau Icefield. The observing station, at 3500 feet, is in the centre of the gently sloping glacier, approximately 2km wide. Rocky ridges with peaks rising above 5000 feet, border the valley. The Taku Glacier is considerably wider. The observing station is again at 3500 ft. in a large flat area 20km from the edge of the icefield. The area is punctuated by occasional rock or snow-covered peaks. It is interesting to note that the winds during measurements at both stations were constantly down-glacier.

The University of New South Wales is about 2km from the ocean on a flat plain marked by old sandhills. The area is covered mainly by residential development and there are large buildings on the campus. The observing station on the tarmac is in an exposed position, but the lawns are sheltered by buildings and trees. High winds were blowing during the University experiments, and even led to the early abandonment of measurements over the tarmac.

6. RESULTS.

A selection of results is shown in Figs. 6.5, 6.6. Fig. 6.5 shows the coefficient of refraction derived from reciprocal levelling on the icefield, for various days. Although there is considerable variation from day to day, an apparent diurnal cycle is evident. Fig. 6.6 compares the variation of refraction over the varied surfaces. The results have still to be fully evaluated and analysed.

TABLE I.

Date 1968	Place	Period of Observation		Weather
		Temperatures hrs.	Refraction hrs.	
Aug. 1	Lemon Creek Glacier	1125-1900	-	Mist, very light breeze
Aug. 3	" " "	920-2330	1000-2230	Mist, no wind
Aug. 6	Taku Glacier	1200-2330	1230-2230	Partly cloudy, light wind
Aug. 7	" "	530- 700	600- 730	Drizzle
Aug. 9	" "	530-2330	600-2230	Windless, clear sky
Aug. 10	" "	1530-2330	1630-2200	Light wind, clear sky
Aug. 11	" "	515-1700	630-1700	Windless, clear sky
Sept.29	Car Park, UNSW	1000-1400	1130-1400	High winds
Sept.30	Lawns, UNSW	730-1800	730-1800	Gusty winds, sun and shadow

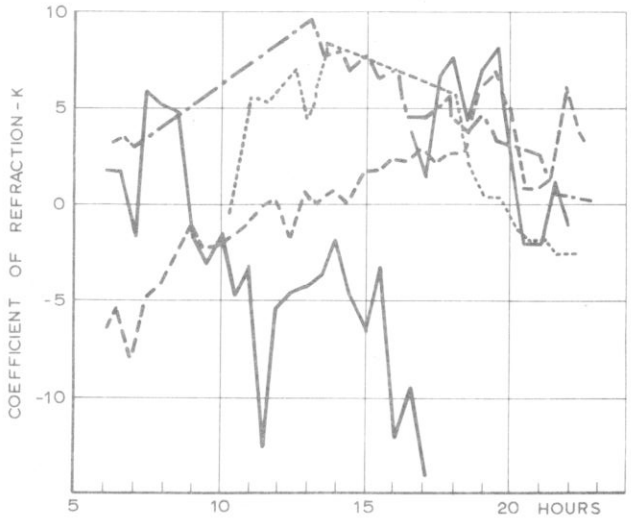

FIGURE 6.5: REFRACTION ON ICEFIELD FROM LEVELLING MEASUREMENTS

Aug. 3
Aug. 6-7
Aug. 9
Aug. 10-11

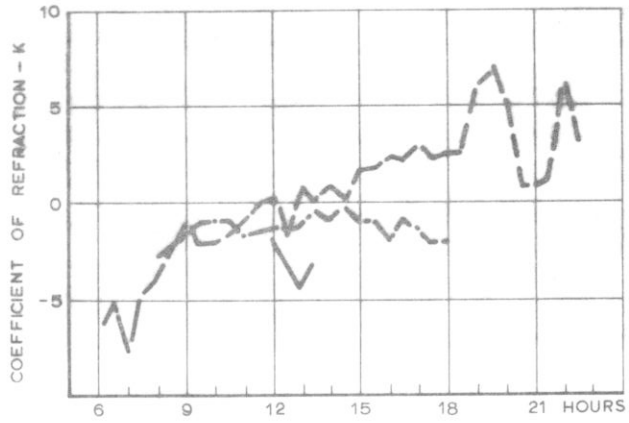

FIGURE 6.6: REFRACTION OVER VARIOUS SURFACES

Icefield, Aug. 9
Grass
Tarmac

7. CONCLUSIONS.

The results show high numerical values of the coefficient of refraction and wide variation. The standard value of K adopted for trigonometric levelling is 0.14 or a value close to this. The measured values show rapid variations not in hundredths but in units of K. In addition there are shorter-term fluctuations which do not show but which were noted during the repetition of observations. During a 40 second period the readings drifted through a whole millimetre, equivalent to a change in K of approximately 3 units, and then returned to their previous values. An observer might take a reading during such a period, find from comparisons that it was apparently inconsistent, repeat the reading to find it differing by a significant amount, and conclude that he had made a mistake.

It is estimated that the standard deviation of K due to errors of observation is between 0.5 and 1.0 on the Icefield and, due to the longer sight length and steadier conditions, below 0.5 in the other experiments. Further analysis is necessary to confirm these figures. Although some of the Icefield results appear to show a diurnal cycle, the pattern is not constant and in fact the variations are apparently due to weather changes. A strong correlation exists between the wind strength and K. The observations over grass show a diurnal cycle, but they would need to be extended over 24 hours to show this fully.

Normal levelling observations take precautions to avoid the effects of refraction, and are so successful in doing so that refraction remains an unknown quantity. The magnitude and variation of K shown by these measurements give cause for a review of other possible hidden effects of refraction. Systematic effects in gaining altitude - foresight always closer to the ground - compensated by a complementary effect in going downhill, are a real possibility. Refraction is ignored in the normal "two-peg adjustment" of a level. In order to take into account the refraction a "three-peg" adjustment is proposed. This involves measurements to a third staff close to the central instrument station. These measurements enable the determination and elimination of refraction effects.

REFERENCE:

ANGUS-LEPPAN, P.V. 1968 — An experimental determination of refraction over an Icefield. UNISURV Report No. 10, University of N.S.W.

PAPER No. 7.

STATISTICAL ANALYSIS OF REFRACTIVE INDEX THROUGH THE TROPOSPHERE AND THE STRATOSPHERE.

Simo H. Laurila

SUMMARY. Tha main environmental problem in ranging to a satellite through the atmosphere is in finding the most probable value of the mean refractive index. In this paper, the mean refractive index is computed as a four-part model. The troposphere is treated as one altitude range from sea level to 9 kilometers, and the stratosphere is divided into three altitude ranges, 9 to 18, 18 to 27, and 27 to 36 kilometers. At 36 kilometers, the N-value is approximately equal to two and reduces rapidly to zero. By the use of the Essen formula in radio wave application and the modified Kohlrausch formula in light wave application, point-to-point values of the refractive index are computed through these altitude ranges. The polynomial expansion of second order from the basic exponential function is selected as the model, and the curve-fitting adjustments of the computed values are established separately to each altitude range to obtain coefficients A, B, and C.

A model based on the U.S. Standard Atmosphere, 1962, is used as the reference to which four sets of actual soundings made in Lihue, Hawaii and Fairbanks, Alaska on February 3 and July 2, 1966, are compared. The results show that the parabolic adjustment has a very high reliability. In the use of standard atmosphere, the standard error of the refractive index through the total altitude range of 0 to 36 kilometers, and at the 70° zenith distance, equals only ±7 millimeters when radio waves are utilized, and ±3 millimeters when light waves are utilized.

1. POINT-TO-POINT DETERMINATION OF THE REFRACTIVE INDEX FOR RADIO WAVES.

The three formulas which follow are commonly used in the determination of the refractive index as a function of the atmospheric parameters--temperature, pressure, and humidity:

Essen Formula:

$$N = (n - 1) \cdot 10^6 = \frac{77.62}{T} P - \left(\frac{12.92}{T} - \frac{37.19 \cdot 10^4}{T^2} \right) e \qquad (1)$$

Essen - Froome Formula:

$$N = (n - 1) \cdot 10^6 = \frac{103.49}{T} (P - e) + \frac{86.26}{T} \left(1 + \frac{5748}{T}\right) e \qquad (2)$$

Smith - Weintraub Formula:

$$N = (n - 1) \cdot 10^6 = \frac{77.6}{T} \left(P + 4.81 \cdot 10^3 \frac{e}{T}\right) \qquad (3)$$

In the Essen and Smith-Weintraub formulas, T is the temperature in Kelvin units, P is the total pressure in millibars, and e is the partial pressure of water vapor in millibars. At the 1960 meeting of the International Union of Goedesy and Geophysics (IUGG, 1960), it was recommended that the Essen-Froome formula be used to achieve uniformity in calculations of electronic distance measurements. It should be noted, however, that the Essen-Froome formula is actually the Essen formula obtained by rearranging terms and stating pressures in millimeters of mercury instead of millibars.

Essen and Smith-Weintraub formulas were compared by applying to both formulas T and P values from the U.S. Standard Atmosphere (1962) and e value from Eq. (5) as follows:

TABLE I.

Comparison of N-Values calculated from formulas.

Altitude, km	Essen, N-Value	Smith-Weintraub, N-value	Difference
0	321.0	321.6	-0.6
1	285.6	286.1	-0.5
2	253.0	253.3	-0.3
3	223.0	223.2	-0.2
4	195.7	195.9	-0.2
5	171.1	171.2	-0.1

Consequently, the use of either formula is justified. In this paper, the Essen formula has been utilized because in actual soundings, the total pressure is given in millibars and the partial pressure of water vapor is given either as the dew point temperature or as the relative humidity. In both cases it is easy to convert them to millibars by using the Smithsonian Meteorological Tables.

2. MODEL OF THE REFRACTIVE INDEX FROM STANDARD ATMOSPHERE.

U.S. Standard Atmosphere (1962) has been selected as the basis for this analysis. Temperature in Kelvin units and total pressure in millibars have been obtained at intervals of 0.5 kilometers from sea level to 36 kilometers. The partial pressure of water vapor was obtained in simultaneous solution of the Essen formula and the parabolic expression of the n-value.

$$n = 1 + A + Bh + Ch^2 \qquad (4)$$

as follows:

$$e = \frac{T^2 \left(\frac{K}{T} P \cdot 10^{-6} - A - Bh - Ch^2\right)}{(TL - M \cdot 10^4)\, 10^{-6}} \tag{5}$$

where $K = 77.62$, $L = 12.92$, and $M = 37.19$. A, B, and C are meteorological constants obtained from the NACA moist atmosphere (JACOBSEN, 1951):

$$\begin{aligned} A &= 0.000321 \\ B &= 0.00003670 \\ C &= 0.000001350 \end{aligned} \tag{6}$$

and h is the geometric height in kilometers.

There are several approaches in forming the model from standard atmosphere; three of them are discussed here.

Henriksen expresses the N-value from zero altitude to the upper limit of the atmosphere by the exponential curve (BROWN, 1965):

$$N = 325 \cdot e^{-.1312 \cdot h \cdot 10^{-3}} \tag{7}$$

where the sea-level value is assumed to be $n_o = 1.000325$, and h is the height above sea level in meters.

Bean expresses the refractive index through atmosphere as a three-part model (BROWN, 1965; BEAN, 1960). He assumes a linear decrease in N for the first kilometer above the station. From 1 to 9 kilometers, he uses the exponential function:

$$N = N_1 \cdot e^{-c\,(h - h_s - 1)} \tag{8}$$

where $c = \frac{1}{8 - h_s} \times \ln \frac{N_1}{105}$, and h_s is the height of the station in kilometers. Above 9 kilometers, the following exponential formula is utilized:

$$N = 105 \cdot e^{-.1424\,(h - 9)} \tag{9}$$

The author presents the refractive index through the atmosphere as a four-part model. The second order parabolic development of the basic exponential function is applied as one altitude range through the troposphere, and as three separate altitude ranges through the stratosphere. Seventy-three values from the U.S. Standard Atmosphere (1962) for T and P were used together with the e-values from Eq. (5), and were adjusted separately for the four altitude ranges, 0 to 9, 9 to 18, 18 to 27, and 27 to 36 kilometers. Curve-fitting adjustment of Essen values into the parabola, Eq. (4), yielded the constants in Table II.

TABLE II.

Constants from curve fitting

Altitude Range, km	A	B	C
0 - 9	0.0003212	-0.000037141	0.0000014370
9 - 18	0.0001062	-0.000013897	0.0000005693
18 - 27	0.0000267	-0.000003786	0.0000001766
27 - 36	0.0000064	-0.000000870	0.0000000380

In Table III, residuals after the adjustment are given at intervals of 1 kilometer from 0 to 15 kilometers, and at intervals of 5 kilometers from 15 to 35 kilometers. E denotes the Essen point-to-point values, and L denotes the values read from the adjusted parabolas.

TABLE III.

Residuals after Adjustment

Altitude, km	E, N-Value	L, N-Value	Residual N-Value	Altitude, km	E, N-Value	L, N-Value	Residual N-Value
0	321.0	321.2	-0.2	11	81.3	80.7	+0.6
1	285.6	285.5	+0.1	12	69.5	69.6	-0.1
2	253.0	252.6	+0.4	13	59.5	59.7	-0.2
3	223.0	222.7	+0.3	14	50.9	50.9	±0
4	195.7	195.6	+0.1	15	43.3	43.3	±0
5	171.1	171.4	-0.3	20	19.7	19.8	-0.1
6	149.3	150.2	-0.9	25	8.8	8.9	-0.1
7	131.4	131.6	-0.2	30	4.1	4.2	-0.1
8	117.3	116.1	+1.2	35	2.0	1.8	+0.2
9	104.1	103.3	+0.8				
10	92.1	92.9	-0.8				

3. STRENGTH OF THE PARABOLIC ASSUMPTION.

In the utilization of refractive index through the atmosphere for satellite tracking, the best-fitting mean refractive index through various altitude ranges is more significant than the point-to-point values. Therefore, instead of the use of Eq. (4), its mean value should be used, as obtained from the following expression:

$$\bar{n} = \frac{1}{h} \int_0^h n \, dh \tag{10}$$

or

$$\bar{n} = A + \frac{h}{2} B + \frac{h^2}{3} C \tag{11}$$

Also, the most realistic criterion in investigating the reliability, or validity, of such mean refractive indexes is to compute the standard error of function (11). According to the general error propagation it will be :

$$m_n = \pm \mu \sqrt{[FF]} \tag{12}$$

where μ is the standard error of the weight unit, and [FF] is the weight number of function (11) obtained as follows:

$$[FF] = f'^2_A [\alpha\alpha] + 2f'_A f'_B [\alpha\beta] + 2f'_A f'_C [\alpha\gamma] + f'^2_B [\beta\beta] + \\ + 2f'_B f'_C [\beta\gamma] + f'^2_C [\gamma\gamma] \tag{13}$$

$[\alpha\alpha]$, $[\beta\beta]$, and $[\gamma\gamma]$ are the weight numbers and $[\alpha\beta]$, $[\alpha\gamma]$, and $[\beta\gamma]$ are the correlation numbers of unknowns A, B, and C. Partial derivatives for the unknowns are denoted by f'_A, f'_B, and f'_C, correspondingly. When applied to Eq. (11), the following expression for [FF] can be written:

$$[FF] = [\alpha\alpha] + h\,[\alpha\beta] + \frac{2}{3}h^2[\alpha\gamma] + \frac{h^2}{4}[\beta\beta] + \frac{h^3}{3}[\beta\gamma] + \frac{h^4}{9}[\gamma\gamma] \qquad (14)$$

Various zenith distances in the tracking of satellites also should be anticipated. Because of the short distances involved, the various altitude ranges are considered as parallels to the flat earth, and the tracking distance S as a function of the altitude range h can be written:

$$S = \frac{h}{\cos\psi} \qquad (15)$$

where ψ is the zenith angle.

Corresponding to the zenith angles, $\psi = 0^\circ$, 30°, 50°, 60°, and 70°, the tracking distances, equivalent to the 9-kilometer altitude range, are S = 9.0, 10.4, 14.0, 18.0 and 26.3 kilometers.

The standard errors of the function (11) at the given angles are presented in Table IV, converted to meters.

TABLE IV.

Standard errors in range due to parabolic assumption - Meters.

Altitude Range, km / Zenith Angle	70°	60°	50°	30°	0°
0 - 9	±0.005	+0.003	±0.002	±0.002	±0.002
9 - 18	0.003	0.002	0.001	0.001	0.001
18 - 27	0.002	0.001	0.001	0.000	0.000
27 - 36	0.001	0.000	0.000	0.000	0.000
0 - 36	0.007	0.004	0.002	0.002	0.002

The largest standard error at the poorest zenith angle, $\psi = 70^\circ$, and through the most vulnerable altitude range, 0 to 9 kilometers, where moisture is present, is only ± 5 millimeters; which, together with the small residuals (in Table III) prove the parabolic curve-fitting adjustment to be very reliable.

4. MODEL OF THE REFRACTIVE INDEX FROM ACTUAL METEOROLOGICAL SOUNDINGS.

The effect of the use of actual meteorological soundings in the vicinity of the tracking station was investigated by selecting four widely separated climatological samples as references. Soundings were obtained at Lihue, Kauai, State of Hawaii, July 2, 1966; Lihue, February 3, 1966; Fairbanks, State of Alaska, July 2, 1966; and Fairbanks, February 3, 1966. All soundings were made at 00.00 Greenwich time.

These samples represented hot and humid, cool and dry, and cold and dry climatological conditions, with the rather anomalous temperature distribution as shown in Table V, given in centigrades:

TABLE V.

Temperature Distribution from Soundings.

Altitude, km	Lihue July	Lihue February	Fairbanks July	Fairbanks February	U.S. Standard
0.5	21	17	23	- 8	12
5.0	0	- 5	-15	-30	-17
10.0	-38	-35	-43	-54	-50
15.0	-69	-71	-45	-46	-57
17.0	-69	-75	-45	-47	-57

All sounding altitudes were given as geopotential heights, which were converted into geometric heights by use of the Smithsonian Meteorological Tables, based on the following formula:

$$h = \frac{M \cdot Z}{\frac{(g\phi \cdot M)}{9.8} - Z} \tag{16}$$

where Z is the geopotential height, $g\phi$ is the actual acceleration of gravity at latitude ϕ, and M is the meridian curvature radius of that latitude.

After this conversion, actual sounding data were applied to the Essen formula, Eq. (1) and then were adjusted into the parabola, Eq. (4) for altitude ranges 0 to 9, 9 to 18, 18 to 27, and 27 to 36 kilometers. The standard errors of the mean refractive index through each altitude range were analyzed in a manner similar to that presented in Table IV, and also the differences between the standard atmosphere and the actual atmosphere were calculated in the unit of meters of distance. The results are given in Tables VI - IX.

5. REFRACTIVE INDEX FOR LIGHT WAVES.

For light waves, the group refractive index is first computed by use of the Barrel and Sears formula as follows (DENISON, 1967):

$$(n_g - 1) \cdot 10^7 = A + \frac{3B}{\lambda^2} + \frac{5C}{\lambda^4} \tag{17}$$

where

$$\begin{aligned} A &= 2876.04 \\ B &= 16.288 \\ C &= 0.131 \end{aligned} \tag{18}$$

In the utilization of a ruby laser, the wavelength $\lambda = 6943$ Å is applied to Eq. (17) and yields the value of the group refractive index as:

$$(n_g - 1) \cdot 10^6 = 297.99 \tag{19}$$

TABLE VI.

Comparison between Computed and Actual Atmosphere. Range measured by Radio Waves

Lihue, July 2 — Total Altitude Range 0.036 to 36.565 km — 35 Soundings

Zenith Angle	0 to 9 km		9 to 18 km		18 to 27 km		27 to 36 km		0 to 36 km	
	St. Error meters	Differ. m	St. Error m	Differ. m	St. Error m	Differ. m	St. Error m	Differ. m	St. Error m	Differ. m
0°	±0.019	-0.005	±0.002	+0.042	±0.000	+0.009	±0.000	±0.000	±0.019	+0.046
30°	0.022	-0.005	0.002	+0.048	0.001	+0.010	0.000	0.000	0.022	+0.053
50°	0.029	-0.009	0.003	+0.064	0.001	+0.014	0.000	0.000	0.029	+0.069
60°	0.036	-0.014	0.004	+0.082	0.001	+0.018	0.001	0.000	0.036	+0.086
70°	0.055	-0.016	0.006	+0.121	0.002	+0.026	0.001	0.000	0.056	+0.131

TABLE VII.

Comparison between Computed and Actual Atmosphere. Range measured by Radio Waves

Lihue, February 3 — Total Altitude Range 0.036 to 33.540 km — 34 Soundings

Zenith Angle	0 to 9 km		9 to 18 km		18 to 27 km		27 to 36 km		0 to 36 km	
	St. Error meters	Differ. m	St. Error m	Differ. m	St. Error m	Differ. m	St. Error m	Differ. m	St. Error m	Differ. m
0°	±0.019	0.067	±0.001	+0.030	±0.000	+0.007	±0.000	-0.001	±0.019	-0.031
30°	0.022	-0.077	0.001	+0.034	0.000	+0.008	0.000	-0.001	0.022	-0.036
50°	0.029	-0.104	0.002	+0.046	0.001	+0.011	0.000	-0.002	0.029	-0.049
60°	0.038	-0.133	0.002	+0.059	0.001	+0.014	0.000	-0.002	0.038	-0.062
70°	0.055	-0.195	0.003	+0.089	0.002	+0.021	0.000	-0.003	0.055	-0.088

TABLE VIII.

Comparison between Computed and Actual Atmosphere Range measured by Radio Waves.

Fairbanks, July 2 — Total Altitude Range 0.499 to 34.720 km — 31 Soundings

Zenith Angle	0 to 9 km		9 to 18 km		18 to 27 km		27 to 36 km		0 to 36 km	
	St. Error m	Differ. m	St. Error m	Differ. m	St. Error m	Differ. m	St. Error m	Differ. m	St. Error m	Differ. m
0^{o}	±0.003	-0.106	±0.003	-0.001	±0.000	+0.005	±0.000	+0.005	±0.005	-0.097
30^{o}	0.003	-0.123	0.003	-0.001	0.000	+0.007	0.000	+0.007	0.004	-0.110
50^{o}	0.004	-0.165	0.004	-0.002	0.000	+0.011	0.000	+0.011	0.006	-0.145
60^{o}	0.006	-0.212	0.005	-0.002	0.000	+0.014	0.001	+0.014	0.008	-0.186
70^{o}	0.008	-0.310	0.008	-0.002	0.000	+0.016	0.001	+0.016	0.011	-0.280

TABLE IX.

Comparison between Computed and Actual Atmosphere Range measured by Radio Waves.

Fairbanks, February 3 — Total Altitude Range 0.146 to 31.362 km — 34 Soundings

Zenith Angle	0 to 9 km		9 to 18 km		18 to 27 km		27 to 36 km		0 to 36 km	
	St. Error m	Differ. m	St. Error m	Differ. m	St. Error m	Differ. m	St. Error m	Differ. m	St. Error m	Differ. m
0^{o}	±0.008	-0.055	±0.003	-0.052	±0.000	-0.004	±0.000	±0.000	±0.009	-0.111
30^{o}	0.010	-0.063	0.003	-0.060	0.000	-0.004	0.001	0.000	0.011	-0.127
50^{o}	0.013	-0.085	0.004	-0.081	0.001	-0.006	0.001	0.000	0.014	-0.172
60^{o}	0.016	-0.110	0.005	-0.104	0.001	-0.007	0.002	0.000	0.017	-0.221
70^{o}	0.024	-0.160	0.008	-0.152	0.001	-0.011	0.002	0.000	0.026	-0.323

To compute the ambient refractive index for light waves, the Kohlrausch formula is usually used, as follows:

$$N = (n - 1) \cdot 10^6 = \frac{n_g - 1}{1 + \alpha t} \cdot \frac{P}{760} - \frac{0.000000055 \cdot e}{1 + \alpha t} \quad 10^6 \qquad (20)$$

where P is the total pressure in millimeters of mercury, e is the partial pressure of water vapor in millimeters of mercury, α is the heat expansion coefficient of air and equals 0.00367 and t is the temperature in centigrade.

Since in actual soundings the total pressure is given in millibars, the author has modified Eq. (20) to be more suitable for computer programming in the following way:

$$N = (n - 1) \cdot 10^6 = \frac{298.0 \cdot P - 41.8 \cdot e}{3.709 \cdot T} \qquad (21)$$

where P and e are given in millibars, and T is the temperature in Kelvin units. In the derivation of Eq. (21) it was anticipated that $T_o = 273.15$, which yields the heat expansion coefficient $\alpha = 0.00366$.

In a manner similar to that presented in connection with radio waves, T and P from U.S. Standard Atmosphere, and e from Eq. (5) were applied to Eq. (21) to obtain point-to-point values for the refractive index of light-wave propagation. Curve-fitting adjustment of these values into the parabola, Eq. (4), yielded the constants in Table X.

TABLE X

Constants from Curve Fitting - Light Waves.

Altitude Range, km	A	B	C
0 - 9	0.0002818	-0.000026408	0.0000007964
9 - 18	0.0001085	-0.000013852	0.0000005465
18 - 27	0.0000279	-0.000003998	0.0000001877
27 - 36	0.0000066	-0.000000907	0.0000000400

TABLE XI.

Residuals after Adjustment

Altitude, km	L, N-Value	P, N-Value	Residual N-Value	Altitude km	L, N-Value	P N-Value	Residual N-Value
0	282.0	281.8	+0.2	10	95.3	95.1	+0.2
1	256.1	256.2	-0.1	11	84.1	83.0	+1.1
2	231.9	232.2	-0.3	12	71.9	71.8	+0.1
3	209.4	209.8	-0.4	13	61.5	61.9	-0.4
4	189.0	188.9	+0.1	14	52.6	52.9	-0.3
5	169.6	169.6	±0	15	44.9	45.1	-0.2
6	152.2	152.0	+0.2	20	20.4	20.7	-0.3
7	136.1	135.9	+0.2	25	9.1	9.1	±0
8	121.4	121.4	±0	30	4.3	4.3	±0
9	107.7	108.5	-0.8	35	1.9	1.9	±0

In Table XI, residuals (after adjustment) are given in N-units, and in Table XII the standard errors through the previously used altitude ranges are given in meters of distance.

TABLE XII.

Standard Errors in Range due to Parabolic Assumption - Meters.

Altitude Range, km	Zenith Angle	70^{o}	60^{o}	50^{o}	30^{o}	0^{o}
0 - 9		±0.001	±0.001	±0.001	±0.000	±0.000
9 - 18		0.003	0.002	0.002	0.001	0.001
18 - 27		0.001	0.001	0.000	0.000	0.000
27 - 36		0.000	0.000	0.000	0.000	0.000
0 - 36		0.003	0.002	0.002	0.001	0.001

The standard errors of the mean refractive index, based on the utilization of the actual soundings, together with the differences between the actual atmosphere and the standard atmosphere, are given in Tables XIII-XVI, converted to meters of distance.

Due to limited number of samples analyzed, no final conclusion can be drawn. However, a very clear correlation exists between standard errors obtained in a hot and humid climate (Hawaii) and in a cold and dry climate (Alaska) when radio-wave propagation is utilized. The total standard errors from sea level to 36 kilometers were ± 6cm and ± 6cm, based on soundings made in Hawaii, and ± 1 cm and ± 3 cm, based on soundings made in Alaska.

The largest difference between distances based on standard-atmosphere data and local-atmosphere data (Fairbanks, February 3, 1966) was -32 cm, which shows that to achieve the ultimate accuracy in utilizing the radio-wave propagation, soundings should be used that have been made in the vicinity or proximity of the tracking station.

In the use of laser and, consequently, light-wave propagation, the influence of humidity is practically negligible. Therefore,standard errors obtained in measurements based on either humid-or dry-climate soundings are of the same order. Due to the absence of the humidity effect, the accuracy of laser tracking is significantly higher than tracking by radio-waves. At the zenith angle $\psi = 70^{o}$, and through the altitude range of 0 to 9 kilometers, the standard error of the mean refractive index based on the U.S. Standard Atmosphere is only ± 1 millimeter. The largest standard error for the total altitude range from 0 to 36 kilometers (Fairbanks, February 3, 1966), was ± 4.2 cm, while the difference between distances based on the standard and local atmospheres was + 3.8 cm. This, together with data obtained from Tables XIII-XVI, suggests that properly selected and computed standard atmosphere values guarantee sufficient accuracy to most geodetic and geophysical applications when light waves are utilized.

ACKNOWLEDGMENT.

This work was supported by the U.S. National Aeronautics and Space Administration under contract NGR 12 - 001 - 045.

TABLE XIII.

Comparison between Computed and Actual Atmosphere Range measured by Light Waves.

Lihue, July 2 — Total Altitude Range 0.036 to 36.565 km — 35 Soundings

Zenith Angle	0 to 9 km		9 to 18 km		18 to 27 km		27 to 36 km		0 to 36 km	
	St. Error meters	Differ. m	St. Error m	Differ. m	St. Error m	Differ. m	St. Error m	Differ. m	St. Error m	Differ. m
0^{o}	±0.004	-0.040	±0.002	+0.045	±0.001	+0.009	±0.000	+0.001	±0.005	+0.015
30^{o}	0.005	-0.046	0.002	+0.052	0.001	+0.010	0.000	+0.001	0.005	+0.017
50^{o}	0.007	-0.062	0.003	+0.070	0.001	+0.014	0.001	+0.001	0.008	+0.023
60^{o}	0.009	-0.079	0.004	+0.090	0.001	+0.018	0.001	+0.002	0.010	+0.031
70^{o}	0.013	-0.116	0.005	+0.132	0.002	+0.026	0.001	+0.003	0.014	+0.045

TABLE XIV.

Comparison between Computed and Actual Atmosphere Range measured by Light Waves.

Lihue, February 3 — Total Altitude Range 0.036 to 33.540 km — 34 Soundings

Zenith Angle	0 to 9 km		9 to 18 km		18 to 27 km		27 to 36 km		0 to 36 km	
	St. Error meters	Differ. m	St. Error m	Differ. m	St. Error m	Differ. m	St. Error m	Differ. m	St. Error m	Differ. m
0^{o}	±0.003	-0.035	±0.001	+0.031	±0.000	+0.006	±0.000	+0.001	±0.003	+0.003
30^{o}	0.004	-0.041	0.002	+0.036	0.000	+0.007	0.000	+0.001	0.004	+0.003
50^{o}	0.005	-0.055	0.002	+0.049	0.000	+0.010	0.000	+0.001	0.005	+0.005
60^{o}	0.007	-0.070	0.003	+0.063	0.001	+0.013	0.000	+0.002	0.008	+0.008
70^{o}	0.010	-0.103	0.004	+0.092	0.001	+0.018	0.000	+0.003	0.011	+0.010

TABLE XV.

Comparison between Computed and Actual Atmosphere Range measured by Light Waves.

Fairbanks, July 2 — Total Altitude Range 0.499 to 34.720 km — 31 Soundings

Zenith Angle	0 to 9 km		9 to 18 km		18 to 27 km		27 to 36 km		0 to 36 km	
	St. Error meters	Differ. m	St. Error m	Differ. m	St. Error m	Differ. m	St. Error m	Differ. m	St. Error m	Differ. m
0^{o}	±0.002	-0.032	±0.003	-0.002	±0.000	+0.005	±0.000	+0.005	±0.004	-0.024
30^{o}	0.003	-0.036	0.004	-0.002	0.000	+0.005	0.001	+0.005	0.005	-0.028
50^{o}	0.004	-0.049	0.005	-0.003	0.000	+0.007	0.001	+0.007	0.007	-0.038
60^{o}	0.005	-0.063	0.006	-0.004	0.001	+0.009	0.001	+0.009	0.008	-0.049
70^{o}	0.007	-0.092	0.009	-0.005	0.001	+0.013	0.001	+0.013	0.012	-0.071

TABLE XVI.

Comparison between Computed and Actual Atmosphere Range measured by Light Waves.

Fairbanks, February 3 — Total Altitude Range 0.146 to 31.362 km — 31 Soundings

Zenith Angle	0 to 9 km		9 to 18 km		18 to 27 km		27 to 36 km		o to 36 km	
	St. Error meters	Differ. m	St. Error m	Differ. m	St. Error m	Differ. m	St. Error m	Differ. m	St. Error m	Differ. m
0^{o}	±0.014	+0.059	±0.004	-0.043	±0.000	-0.006	±0.001	+0.002	±0.015	+0.012
30^{o}	0.015	+0.069	0.004	-0.050	0.000	-0.006	0.002	+0.002	0.016	+0.015
50^{o}	0.021	+0.092	0.005	-0.067	0.000	-0.008	0.002	+0.003	0.022	+0.020
60^{0}	0.027	+0.119	0.007	-0.086	0.001	-0.011	0.003	+0.004	0.028	+0.026
70^{o}	0.040	+0.173	0.010	-0.124	0.001	-0.016	0.004	+0.005	0.042	+0.038

REFERENCES:

INTERNATIONAL UNION OF GEODESY & GEOPHYSICS 1960 — Resolution, General Assembly, Helsinki. Bull. Geodesique. No. 58.

U.S. STANDARD ATMOSPHERE 1962 — U.S. Government Printing Office, Washington. D.C.

JACOBSEN, C.E. 1951 — High Precision Shoran Test, Phase I. AF Tech. Report. No. 6611, U.S. Air Force.

BROWN, W.W. 1965 — The Reflection Problem in Distance Measurements to Artificial Satellites. Special Report. Ohio State University, Department of Geodetic Science (Unpublished).

BEAN, B.R. 1960 — Atmospheric Bending of Radio Waves. Electromagnetic Wave Propagation, M. Desirant and J.L. Michiels (Editors), Academic Press, New York.

DENISON, E.W. 1967 — Report of Special Study Group No. 19: Electromagnetic Distance Measurement, 1963-1967. Int. Assn. Geodesy.

DISCUSSION: PAPERS 5, 6 and 7.

Chairman: Mr. M. Puttock

BROWN: Refraction Measurements

ANGUS-LEPPAN: Refraction in Levelling

LAURILA: Stratospheric Refraction.

MacLEAN: Referring to Brown's paper, Fig. 12, is there any significance in the break in measurements during the evening, and the large change in refraction?

BROWN: The refraction angles are much larger at night, due to the formation of inversions. The break in readings occurred when the observers rested.

KIRSCH: How are the results of the experiments applied in practice?

BROWN: The experiments showed that temperature measurements were the most satisfactory. When a rocket was fired these measurements were made on towers for the lowest layers and from weather balloons for higher layers. The refraction correction was calculated from these temperature readings.

GALE: Would Angus-Leppan give some details of the mathematical model which he mentioned?

ANGUS-LEPPAN: My aim is to develop a more sophisticated standard atmosphere which takes into account variations in altitude and time of day; it is in the form of an equation with constants, whose values depend on climate, season, cloudiness and other factors. So far a form for the temperature gradient has been developed:

$$G = g_o + a_1 z + a_2 e^{-a_3 z} + a_4 e^{-a_5 z} \{a_6 \sin(t + a_7) + a_8 \sin(2t + a_9)\}$$

t = time of day. 24 hours = 360^o

z = height above surface

This form appears to cope with a wide variety of conditions, with different values of the constants g_o, a_1 - a_9. Other speakers might comment on the form.

WEBB: I do not think that this is the form I would have chosen. The theory outlined in my paper (No. 1) would suggest modifications and improvements in the form of some of the terms.

McMAHON: What equipment was used by Laurila for temperature and humidity?

LAURILA: As indicated in my paper I made no special measurements. Results of the routine radiosonde balloon ascents carried out by the U.S. Weather Bureau were used.

OWENS: How does Laurila define his standard error?

LAURILA: It is a measure of the fit of the standard atmosphere to the parabola derived by me.

OWENS: Because the errors are so small the form assumed for the atmosphere, whether standard or measured profile, is not critical.

LYONS: Field observations in trigonometric levelling are over long distances. Why does Angus-Leppan use short lines and are the results applicable to long lines?

ANGUS-LEPPAN: The aim in the experiments is to limit the number of variables. Over well-chosen short lines the effect of surface and topography are likely to be constant. Results obtained over short lines are certainly applicable over longer lines though the effects are complicated by the multiplicity of conditions. It is necessary to divide a longer line into sections with constant conditions and integrate the refraction over all sections. However the most effective practical approach is still to observe simultaneous reciprocal angles.

BROWN: In our experiments we obtained a good correlation between the temperature observations at a point and the refraction on lines which were ten miles away.

GALE: Experience in Canada shows that it is important to observe reciprocal vertical angles at precisely the same time. Both observers are usually in contact by radio and at a chosen time both make observations.

(A similar procedure is adopted by the Trigonometrical Survey of South Africa. Observers commence observations at the same moment and both stop at the same time irrespective of the number of observations. Two way radio contact by walkie-talkie or tellurometer is essential. See Proc. Third Nat. Conf. S.African Surveyors, Paper No.7/27 - Ed.)

ANGUS-LEPPAN: The ideal will be some device for measuring the reciprocal refraction by means of observations at only one end of the line. There is some hope that this will be possible by means of a reflection system being tested at the University of New South Wales.

KIRSCH: What about the movements of the instrument towers in Brown's experiments for measuring the refraction : were the effects significant?

BROWN: Tests showed the linear movements of the towers were negligible, but they could cause rotation of the camera used for measuring the refraction. This is why the measurements taken are the difference between the position of a near target and a distant target.

BROUGHTON: In Fig. 12 of Brown's paper a shift of the measured refraction graphs 30 minutes earlier (to the left) produces a better fit. Can this be explained?

BROWN: I have no explanation.

ANGUS-LEPPAN: The temperature gradients were measured at one position, whereas the refraction was an integrated value over the length of the line. The air mass is moving more or less as a block (though there is a shearing effect due to surface friction) and possibly the air mass took one half hour to move from the site of temperature measurement to roughly the centre of the line where it represented average conditions over the length. This could be checked from wind records

WEBB: In Brown's paper, refraction is given in Fig. 2 as seconds per 1000 feet, and in Fig. 8 in refractive index gradient. What is the relationship?

BROWN: Curvature of 1 sec. per 1000 feet is 5×10^{-4} (radians/1000 feet). Curvature is also given by $\frac{1}{\mu}\frac{d\mu}{dh} \doteq \frac{d\mu}{dh}$ where μ is the refractive index. A gradient of the index equivalent to the curvature of 6×10^{-6} (radians/1000 feet) is shown in Fig. 8.

McMAHON: What is the horizontal component of refraction at nine miles?

BROWN: We have not studied this.

(Although it is easy to measure changes in lateral refraction it is extremely difficult to obtain absolute values. Estimates can be obtained from triangular closures, and reciprocal azimuth measurements as in the traverses of the Geodetic Survey of Australia, but in these cases the effects are overlaid with other errors. - Ed.)

KIRSCH: In unfavourable observing conditions of a steep-sided valley and near-grazing rays, considerable variation was observed - up to 15 secs. - on a line 4500 feet long, with intermittent cloud.

In tunnels there is a temperature gradient from the walls towards the centre and this is modified at the tunnel mouth. Tests in Snowy Mountains tunnels have shown that lines observed centrally along a tunnel are substantially free of lateral refraction. If for practical reasons the centre cannot be used, a double traverse with lines of sight criss-crossing the tunnel symmetrically eliminates the effect. On lines of 4000 feet, refraction as high as 14" has been measured close to the walls, though 4" would be closer to the average.

ANGUS-LEPPAN: In measuring air temperature, thermocouples or metal resistance elements seem to be favoured. Why are thermistors not used. Their high coefficient of resistance with temperature changes is a major advantage.

THWAITE: Thermistors have non-linear characteristics and there has been doubt, in the past, about their stability.

WEBB: Non-linearity is not a problem if temperature differences are being measured.

ANGUS-LEPPAN: Rigid U.S. Geological Survey testing has shown them to be very stable